

Double-mixing CP violation in B decays

Wen-Jie Song, Yin-Fa Shen and Qin Qin

School of Physics, Huazhong University of Science and Technology, Wuhan 430074, China

E-mail: jaysong@hust.edu.cn, syf70280@hust.edu.cn, qqin@hust.edu.cn

ABSTRACT: We study a long-overlooked CP violation observable, termed double-mixing CP violation, which arises from the interference between two neutral meson oscillating paths involved in a decay chain. The double-mixing CP violation is beneficial for the precise test of the Standard Model CKM mechanism, as it offers the potential to extract weak phases without pollution from strong dynamics. To provide a comprehensive understanding of the double-mixing CP violation, we perform phenomenological analyses on the cascade decays of the B_d^0 and B_s^0 mesons. Our results show that the double-mixing CP violation can be very significant in certain decay channels, such as $B_s^0 \rightarrow \rho^0 K \rightarrow \rho^0(\pi^- \ell^+ \nu_\ell)$. In addition, we employ the decay process $B_d^0 \rightarrow D^0 K \rightarrow (K^- \pi^+)(\pi \ell \nu)$ to demonstrate that the involved strong and weak phases can be directly determined from the experimental data without any theoretical inputs.

Contents

1	Introduction	2
2	Formulae	3
3	Numerical analysis	9
3.1	B_d^0 decays	9
3.1.1	$B_d^0 \rightarrow J/\psi K \rightarrow J/\psi(\pi^\pm \ell^\mp \nu)$	10
3.1.2	$B_d^0 \rightarrow J/\psi K \rightarrow J/\psi f_+$	12
3.1.3	$B_d^0 \rightarrow DK \rightarrow (K^- \pi^+)(\pi^+ \ell^- \bar{\nu}_\ell)$	14
3.1.4	$B_d^0 \rightarrow DK_S^0 \rightarrow f_+ K_S^0$	16
3.1.5	$B_d^0 \rightarrow DK_S^0 \rightarrow (K^- \pi^+) K_S^0$	17
3.2	B_s^0 decays	19
3.2.1	$B_s^0 \rightarrow J/\psi K \rightarrow J/\psi f_+$	20
3.2.2	$B_s^0 \rightarrow J/\psi K \rightarrow J/\psi(\pi^\pm \ell^\mp \nu_\ell)$	20
3.2.3	$B_s^0 \rightarrow \rho^0 K \rightarrow \rho^0(\pi^\pm \ell^\mp \nu)$	23
3.2.4	$B_s^0 \rightarrow DK \rightarrow (K^- \pi^+)(\pi^- \ell^+ \nu_\ell)$	26
3.2.5	$B_s^0 \rightarrow DK_S^0 \rightarrow (\pi^+ \pi^-) K_S^0$ and $B_s^0 \rightarrow DK_S^0 \rightarrow (K^- \pi^+) K_S^0$	29
4	Conclusions	30
A	Formulae for Category 3	33

1 Introduction

CP violation plays a crucial role in flavor physics. It is one of the fundamental criteria for explaining the matter-antimatter asymmetry of the universe [1]. However, the standard model (SM) does not account for a sufficiently large CP violation to explain the observed asymmetry [2, 3]. This suggests the presence of additional sources of CP violation beyond the standard Cabibbo-Kobayashi-Maskawa (CKM) mechanism [4, 5]. Consequently, the quest for non-standard CP violation is a vital undertaking in the quark flavor sector. One systematic approach involves testing the unitarity of the CKM matrix, which relies on measurements of CP violation in quark flavor processes to determine the values of the CKM phase angles. Therefore, it is imperative to conduct comprehensive investigations into CP violation in flavor physics, to precisely test and explore potential sources of CP violation beyond the framework of the CKM mechanism.

Since the unexpected discovery of indirect CP violation in the neutral K meson system in 1964 [6], significant theoretical and experimental advancements have been achieved [7–20], including the detection of CP violation in the B and D meson decays [10, 11, 20]. These studies have successfully observed three types of CP violation under the CKM mechanism in meson systems, along with measurements of CP-violating phases and testing of the unitarity of the CKM matrix. As no evidence of non-standard CP violation has been observed yet, collaborative efforts in both theoretical and experimental domains are essential to conduct more precise tests. In general, experimental precision of channels takes advantage of powerful flavor experiments such as BESIII [21], Belle II [22], and LHCb [23–25]. The primary theoretical challenge in improving precision lies in disentangling the effects of strong interactions within the SM and non-standard contributions. Despite numerous studies dedicated to strong interactions (see *e.g.* [26–35]), the theoretical predictions arising from strong interactions still struggle to align well with the current experimental precision. Therefore, there is an anticipation to provide CP violation observables that are less affected or unaffected by strong interactions.

Of the three types of observed CP violation—direct CP violation, CP violation in mixing, and CP violation in interference between a decay without mixing $M^0 \rightarrow f$ and a decay with mixing $M^0 \rightarrow \bar{M}^0 \rightarrow f$ —the last one has the potential to avoid contamination from strong dynamics. The visualization of CP violation induced by the CKM mechanism typically involves interference between amplitudes with distinct CKM phases and CP-conserving phases, often including strong phases. However, the $M^0 \rightarrow f$ and $M^0 \rightarrow \bar{M}^0 \rightarrow f$ amplitudes have a relative CP-conserving phase induced by different time evolution, making strong phases not a necessity. In fact, the first significant CP violation effect observed by B factories in $B_d^0 \rightarrow J/\psi K_S^0$ [10, 11] serves as a representative example of this type. The CP violation in the interference between $i \rightarrow M^0$ and $i \rightarrow \bar{M}^0 \rightarrow M^0$ [36] also capitalizes on the same advantage provided by neutral meson mixing. It motivates us to develop more CP violation observables that involve mixing.

In our recent study [37], we introduced a long-overlooked form of CP violation arising from the interference between two neutral meson oscillating paths involved in a decay chain. Such a decay, involving two neutral mesons $M_{1,2}^0$, typically occurs via two amplitudes:

$M_1^0 \rightarrow M_2^0 \rightarrow \bar{M}_2^0 \rightarrow f$ and $M_1^0 \rightarrow \bar{M}_1^0 \rightarrow \bar{M}_2^0 \rightarrow f$, as depicted in **Figure 1**, where the particles associated with M_2 are hidden for convenience. We refer to this type of CP violation as the double-mixing CP violation. This introduces a new experimental approach, allowing for measuring the dependence of CP violation on two time variables, specifically the evolution periods of $M_{1,2}$. Our previous research [37] revealed that the existence of double-mixing CP violation does not necessarily require a nonzero strong phase, offering the potential to extract weak phases without the influence of strong dynamics. In some cases where a strong phase is involved, it is also feasible to directly extract the strong phase from experimental data, thereby avoiding significant theoretical uncertainties. To provide a more comprehensive understanding, we will explore the double-mixing CP violation in typical B_d^0 and B_s^0 meson cascade decays in this study.

The rest of the paper is organized as follows. In section II, we provide the general formulas for the double-mixing CP violation in the process $M_1^0(t_1) \rightarrow M_2(t_2) \rightarrow f$, where M_2 is either M_2^0 or \bar{M}_2^0 . In section III, we introduce a numerical analysis strategy to calculate the double-mixing CP violation in cascade decays of M_1^0 , where M_1^0 can be either B_d^0 or B_s^0 . Different initial and final states exhibit markedly distinct patterns. With frequently oscillating $B_{(s)}^0$ and K^0 involved, the double-mixing CP violation effects are generally more promising. In the case of semi-leptonic final states, such as $B_d^0 \rightarrow J/\psi K \rightarrow J/\psi(\pi\ell\nu)$, the total CP violation predominantly stems from contributions of the double-mixing CP violation. Conversely, the contribution of the double-mixing CP violation is exceedingly small when D^0 is involved, primarily due to the negligible mixing of D^0 . We employ certain decay processes, such as $B_s^0 \rightarrow \rho^0 K \rightarrow \rho^0(\pi^\pm \ell^\mp \nu_\ell)$, to reveal that the double-mixing CP violation is possibly significantly large, exceeding 50%. These decay modes could serve as the initial experimental attempts to search for the double-mixing CP violation. Of greater significance, the double-mixing CP violation in certain decay channels under investigation can be utilized for CKM phase extraction, such as in the case of $B_d^0 \rightarrow D^0 K \rightarrow (K^- \pi^+)(\pi\ell\nu)$. Despite involving both strong and weak phases simultaneously, both phases can be extracted through experimental measurements of the double-mixing CP violation without relying on any theoretical inputs. In section IV, we summarize our results and present a conclusion.

2 Formulae

We adopt the conventional formulae that the mass eigenstates $M_{H,L}$ of the flavored neutral mesons are superpositions of their flavor eigenstates M^0 and \bar{M}^0 [38],

$$|M_{H,L}\rangle = p |M^0\rangle \mp q |\bar{M}^0\rangle, \quad (2.1)$$

where q, p are complex coefficients. Then, the time evolution starting from a flavor eigenstate in the case of CPT conservation is given by,

$$\begin{aligned} |M^0(t)\rangle &= g_+(t) |M^0\rangle - \frac{q}{p} g_-(t) |\bar{M}^0\rangle, \\ |\bar{M}^0(t)\rangle &= g_+(t) |\bar{M}^0\rangle - \frac{p}{q} g_-(t) |M^0\rangle, \end{aligned} \quad (2.2)$$

where the functions $g_{\pm}(t)$ of time are given by

$$g_{\pm}(t) = \frac{1}{2} \left[\exp \left(-im_H t - \frac{1}{2}\Gamma_H t \right) \pm \exp \left(-im_L t - \frac{1}{2}\Gamma_L t \right) \right], \quad (2.3)$$

with $m_{H(L)}$ and $\Gamma_{H(L)}$ being the mass and decay width of the ‘Heavy(Light)’ mass eigenstate $M_{H(L)}$, respectively.

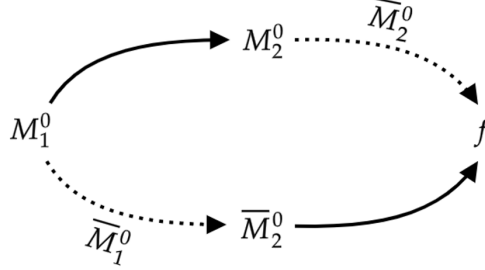


Figure 1. Two oscillation paths in the cascade decay $M_1^0 \rightarrow M_2 \rightarrow f$ with only $M_1^0 \rightarrow M_2^0$, $\bar{M}_2^0 \rightarrow f$ and their CP conjugate processes being allowed. The decay products associated with M_2 are not displayed.

The double-mixing CP violation will occur in the cascade decay containing at least two different neutral mesons. The process illustrated in **Figure 1** serves as a clear example. During the time interval t_1 , a primary neutral meson M_1^0 either remains in its original state or oscillates into its antiparticle \bar{M}_1^0 , which subsequently decays into a secondary neutral meson $\bar{M}_2^0(M_2^0)$. Other accompanying particles are not shown in the figure for simplicity. Similarly, the intermediate state $M_2(t_2)$, representing a time-evolved neutral meson, $M_2^0(t_2)$ or $\bar{M}_2^0(t_2)$, decays into a final state f . Here, t_2 denotes the time for the oscillation of $M_2^0(\bar{M}_2^0)$ in the rest frame of $M_2^0(\bar{M}_2^0)$. The time-dependent CP asymmetry in the chain $M_1^0(t_1) \rightarrow M_2(t_2) \rightarrow f$ can be defined as

$$\begin{aligned} A_{\text{CP}}(t_1, t_2) &\equiv \frac{|\mathcal{M}|^2(t_1, t_2) - |\bar{\mathcal{M}}|^2(t_1, t_2)}{|\mathcal{M}|^2(t_1, t_2) + |\bar{\mathcal{M}}|^2(t_1, t_2)} = \frac{N(t_1, t_2)}{D(t_1, t_2)}, \\ N(t_1, t_2) &= e^{-\Gamma_1 t_1} \left[C_h(t_2) \cosh \frac{\Delta\Gamma_1 t_1}{2} + C_n(t_2) \cos \Delta m_1 t_1 \right. \\ &\quad \left. + S_n(t_2) \sin \Delta m_1 t_1 + S_h(t_2) \sinh \frac{\Delta\Gamma_1 t_1}{2} \right], \\ D(t_1, t_2) &= e^{-\Gamma_1 t_1} \left[C'_h(t_2) \cosh \frac{\Delta\Gamma_1 t_1}{2} + C'_n(t_2) \cos \Delta m_1 t_1 \right. \\ &\quad \left. + S'_n(t_2) \sin \Delta m_1 t_1 + S'_h(t_2) \sinh \frac{\Delta\Gamma_1 t_1}{2} \right], \end{aligned} \quad (2.4)$$

where the amplitude $\mathcal{M}(t_1, t_2)$ is the sum of amplitudes of all possible paths, while $\bar{\mathcal{M}}(t_1, t_2)$ represents the CP conjugate of $\mathcal{M}(t_1, t_2)$. The differences in widths and masses are defined as $\Delta\Gamma \equiv \Gamma_H - \Gamma_L$ and $\Delta m \equiv m_H - m_L$, respectively, and the average of widths is $\Gamma \equiv (\Gamma_H + \Gamma_L)/2$. Here, the subscripts 1 and 2 denote the primary meson M_1 and the secondary

meson M_2 , respectively. Evidently, according to the t_1 dependence, $N(t_1, t_2)$ and $D(t_1, t_2)$ can be written in four terms. Alternatively, a different t_1 function basis can be chosen, for example, rewriting the two terms in $N(t_1, t_2)$ as

$$e^{-\Gamma_1 t_1} \left[C_h(t_2) \cosh \frac{\Delta\Gamma_1 t_1}{2} + C_n(t_2) \cos \Delta m_1 t_1 \right] \rightarrow C_+(t_2) |g_{+,1}(t_1)|^2 + C_-(t_2) |g_{-,1}(t_1)|^2, \quad (2.5)$$

and the same substitution also applies to $D(t_1, t_2)$.

We will provide the explicit expressions of the terms in (2.4) for different cases. We categorize all cases into three groups based on the number of possible oscillation and decay paths. Besides the two-path scenario shown in **Figure 1**, there are also four- and eight-path ones, which will be discussed in more detail below.

Category 1

In the first category, we consider decay processes that occur via two possible paths, as exemplified in **Figure 1**. In this study, we are only interested in cases where direct CP violation is negligible, so we have $\langle \bar{M}_2^0 | \bar{M}_1^0 \rangle = \langle M_2^0 | M_1^0 \rangle e^{i\omega}$ with ω being a pure weak phase, and $\langle f | \bar{M}_2^0 \rangle = \langle \bar{f} | M_2^0 \rangle$. The mixing parameters of $M_{1,2}$ are written as $(q/p)_{1,2} = |(q/p)_{1,2}| e^{-i\phi_{1,2}}$, with $\phi_{1,2}$ complex phases.

The amplitude $\mathcal{M}(t_1, t_2)$ of the process $M_1^0(t_1) \rightarrow M_2(t_2) \rightarrow f$ and its CP conjugate $\bar{\mathcal{M}}(t_1, t_2)$ are given by

$$\begin{aligned} \mathcal{M}(t_1, t_2) &= \langle f | M_2^0(t_2) \rangle \langle M_2^0 | M_1^0(t_1) \rangle + \langle f | \bar{M}_2^0(t_2) \rangle \langle \bar{M}_2^0 | M_1^0(t_1) \rangle, \\ \bar{\mathcal{M}}(t_1, t_2) &= \langle \bar{f} | M_2^0(t_2) \rangle \langle M_2^0 | \bar{M}_1^0(t_1) \rangle + \langle \bar{f} | \bar{M}_2^0(t_2) \rangle \langle \bar{M}_2^0 | \bar{M}_1^0(t_1) \rangle. \end{aligned} \quad (2.6)$$

Considering the time evolution of the neutral mesons (2.2) - (2.3), we can make the following substitutions

$$\begin{aligned} \langle M_2^0 | M_1^0(t_1) \rangle &= g_{+,1}(t_1) \langle M_2^0 | M_1^0 \rangle, & \langle \bar{M}_2^0 | M_1^0(t_1) \rangle &= -\frac{q_1}{p_1} g_{-,1}(t_1) \langle \bar{M}_2^0 | \bar{M}_1^0 \rangle, \\ \langle \bar{M}_2^0 | \bar{M}_1^0(t_1) \rangle &= g_{+,1}(t_1) \langle \bar{M}_2^0 | \bar{M}_1^0 \rangle, & \langle M_2^0 | \bar{M}_1^0(t_1) \rangle &= -\frac{p_1}{q_1} g_{-,1}(t_1) \langle M_2^0 | M_1^0 \rangle, \\ \langle f | M_2^0(t_2) \rangle &= -\frac{q_2}{p_2} g_{-,2}(t_2) \langle f | \bar{M}_2^0 \rangle, & \langle \bar{f} | M_2^0(t_2) \rangle &= g_{+,2}(t_2) \langle \bar{f} | M_2^0 \rangle, \\ \langle \bar{f} | \bar{M}_2^0(t_2) \rangle &= -\frac{p_2}{q_2} g_{-,2}(t_2) \langle \bar{f} | M_2^0 \rangle, & \langle f | \bar{M}_2^0(t_2) \rangle &= g_{+,2}(t_2) \langle f | \bar{M}_2^0 \rangle. \end{aligned} \quad (2.7)$$

Then, it arrives that the total time-dependent CP asymmetry (2.4).

The corresponding double-mixing CP asymmetry is reflected by the S_h and S_n terms, which are induced by the interference between the upper and lower paths in **Figure 1**. The results are given by

$$\begin{aligned} S_h(t_2) &= \frac{e^{-\Gamma_2 t_2}}{2} \left[\sinh \frac{\Delta\Gamma_2 t_2}{2} \cos(\omega - \phi_1 + \phi_2) \left(\left| \frac{q_1}{p_1} \right| \left| \frac{q_2}{p_2} \right| - \left| \frac{p_1}{q_1} \right| \left| \frac{p_2}{q_2} \right| \right) \right. \\ &\quad \left. + \sin \Delta m_2 t_2 \sin(\omega - \phi_1 + \phi_2) \left(\left| \frac{q_1}{p_1} \right| \left| \frac{q_2}{p_2} \right| + \left| \frac{p_1}{q_1} \right| \left| \frac{p_2}{q_2} \right| \right) \right], \\ S_n(t_2) &= \frac{e^{-\Gamma_2 t_2}}{2} \left[-\sinh \frac{\Delta\Gamma_2 t_2}{2} \sin(\omega - \phi_1 + \phi_2) \left(\left| \frac{p_1}{q_1} \right| \left| \frac{p_2}{q_2} \right| + \left| \frac{q_1}{p_1} \right| \left| \frac{q_2}{p_2} \right| \right) \right. \end{aligned} \quad (2.8)$$

$$+ \sin \Delta m_2 t_2 \cos (\omega - \phi_1 + \phi_2) \left(\left| \frac{q_1}{p_1} \right| \left| \frac{q_2}{p_2} \right| - \left| \frac{p_1}{q_1} \right| \left| \frac{p_2}{q_2} \right| \right). \quad (2.9)$$

The common factors $|\langle M_2^0 | M_1^0 \rangle|^2$ and $|\langle f | \bar{M}_2^0 \rangle|^2$ are omitted in the above expression. The remaining terms in the numerator, which are not the focus of our current discussion, are given by

$$C_+(t_2) = \left(\left| \frac{q_2}{p_2} \right|^2 - \left| \frac{p_2}{q_2} \right|^2 \right) |g_{-,2}(t_2)|^2, \quad C_-(t_2) = \left(\left| \frac{q_1}{p_1} \right|^2 - \left| \frac{p_1}{q_1} \right|^2 \right) |g_{+,2}(t_2)|^2. \quad (2.10)$$

The $C_+(t_2)$ term is contributed by purely the upper path in **Figure 1**, where $M_2^0 \rightarrow \bar{M}_2^0$ oscillation is the only CP violation source, while the $C_-(t_2)$ term is contributed purely by the lower path, where CP violation is induced by $M_1^0 \rightarrow \bar{M}_1^0$ oscillation. The terms contributing to $D(t_1, t_2)$ are given by

$$C'_+(t_2) = \left(\left| \frac{q_2}{p_2} \right|^2 + \left| \frac{p_2}{q_2} \right|^2 \right) |g_{-,2}(t_2)|^2, \quad C'_-(t_2) = \left(\left| \frac{q_1}{p_1} \right|^2 + \left| \frac{p_1}{q_1} \right|^2 \right) |g_{+,2}(t_2)|^2, \quad (2.11)$$

$$S'_h(t_2) = \frac{e^{-\Gamma_2 t_2}}{2} \left[\sinh \frac{\Delta \Gamma_2 t_2}{2} \cos (\omega - \phi_1 + \phi_2) \left(\left| \frac{q_1}{p_1} \right| \left| \frac{q_2}{p_2} \right| + \left| \frac{p_1}{q_1} \right| \left| \frac{p_2}{q_2} \right| \right) \right. \\ \left. + \sin \Delta m_2 t_2 \sin (\omega - \phi_1 + \phi_2) \left(\left| \frac{q_1}{p_1} \right| \left| \frac{q_2}{p_2} \right| - \left| \frac{p_1}{q_1} \right| \left| \frac{p_2}{q_2} \right| \right) \right], \quad (2.12)$$

$$S'_n(t_2) = \frac{e^{-\Gamma_2 t_2}}{2} \left[-\sinh \frac{\Delta \Gamma_2 t_2}{2} \sin (\omega - \phi_1 + \phi_2) \left(\left| \frac{q_1}{p_1} \right| \left| \frac{q_2}{p_2} \right| - \left| \frac{p_1}{q_1} \right| \left| \frac{p_2}{q_2} \right| \right) \right. \\ \left. + \sin \Delta m_2 t_2 \cos (\omega - \phi_1 + \phi_2) \left(\left| \frac{q_1}{p_1} \right| \left| \frac{q_2}{p_2} \right| + \left| \frac{p_1}{q_1} \right| \left| \frac{p_2}{q_2} \right| \right) \right]. \quad (2.13)$$

For the convenience of further analysis, we define the two-dimensional time-dependent double-mixing CP asymmetry $A_{dm}(t_1, t_2)$, which is represented as

$$A_{dm}(t_1, t_2) = \frac{e^{-\Gamma_1 t_1}}{D(t_1, t_2)} \left(S_h(t_2) \sinh \frac{\Delta \Gamma_1 t_1}{2} + S_n(t_2) \sin \Delta m_1 t_1 \right) \quad (2.14)$$

$$= A_{h,dm}(t_1, t_2) + A_{n,dm}(t_1, t_2). \quad (2.15)$$

It represents the double-mixing component within the $A_{CP}(t_1, t_2)$ in (2.4). In fact, the remaining part is negligible.

For decay processes occurring via $M_1^0 \rightarrow \bar{M}_2^0 \rightarrow M_2^0 \rightarrow f$ and $M_1^0 \rightarrow \bar{M}_1^0 \rightarrow M_2^0 \rightarrow f$, the results can be directly obtained by applying the replacement $p_2/q_2 \rightarrow q_2/p_2$ from (2.11) - (2.13), *i.e.*, $|p_2/q_2| \rightarrow |q_2/p_2|$ and $\phi_2 \rightarrow -\phi_2$.

Category 2

In the second category, we consider that f is a CP eigenstate that can decay from both M_2^0 and \bar{M}_2^0 . Unlike **Category 1**, there are four possible paths, as shown in **Figure 2**. Assuming negligible direct CP asymmetries, we can express $\langle \bar{M}_2^0 | \bar{M}_1^0 \rangle = \langle M_2^0 | M_1^0 \rangle e^{i\omega}$, and $\langle f | M_2^0 \rangle = \langle f | \bar{M}_2^0 \rangle$ under a suitable convention. It is important to note that in practical terms, M_2^0 here must be K^0 . If it were D^0 decaying from B mesons, its antiparticle \bar{D}^0 could also decay from the same B meson, rendering this category inapplicable. This justifies

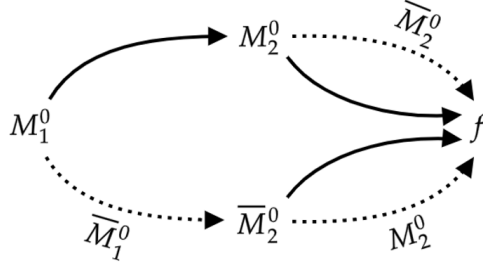


Figure 2. Four oscillation paths in the cascade decay $M_1^0 \rightarrow M_2 \rightarrow f$ where f is a CP eigenstate, with $M_1^0 \rightarrow M_2^0$, $\bar{M}_2^0 \rightarrow f$ and their CP conjugate processes being allowed.

the assumption $\langle f | M_2^0 \rangle = \langle f | \bar{M}_2^0 \rangle$ as CP violation is tiny in strange decays. The result for the CP asymmetry (2.4) is listed below.

To clarify the physical meaning, we separate the S_h and S_n terms in (2.4) into two parts, which are given by

$$S_{n,1}(t_2) = -\frac{e^{-\Gamma_2 t_2}}{2} \left[\left(\left| \frac{q_2}{p_2} \right| + \left| \frac{p_2}{q_2} \right| \right) \sin \Phi \sinh \frac{\Delta \Gamma_2 t_2}{2} - \left(\left| \frac{q_2}{p_2} \right| - \left| \frac{p_2}{q_2} \right| \right) \cos \Phi \sin \Delta m_2 t_2 \right] \times \left(\left| \frac{q_1}{p_1} \right| + \left| \frac{p_1}{q_1} \right| \right), \quad (2.16)$$

$$S_{h,1}(t_2) = \frac{e^{-\Gamma_2 t_2}}{2} \left[\left(\left| \frac{q_2}{p_2} \right| + \left| \frac{p_2}{q_2} \right| \right) \cos \Phi \sinh \frac{\Delta \Gamma_2 t_2}{2} + \left(\left| \frac{q_2}{p_2} \right| - \left| \frac{p_2}{q_2} \right| \right) \sin \Phi \sin \Delta m_2 t_2 \right] \times \left(\left| \frac{q_1}{p_1} \right| - \left| \frac{p_1}{q_1} \right| \right), \quad (2.17)$$

$$S_{n,2}(t_2) = -\left(\left| \frac{p_1}{q_1} \right| + \left| \frac{q_1}{p_1} \right| \right) \left[\sin(\Phi - \phi_2) |g_{+,2}(t_2)|^2 + \sin(\Phi + \phi_2) |g_{-,2}(t_2)|^2 \right], \quad (2.18)$$

$$S_{h,2}(t_2) = \left(\left| \frac{q_1}{p_1} \right| - \left| \frac{p_1}{q_1} \right| \right) \left[\cos(\Phi - \phi_2) |g_{+,2}(t_2)|^2 + \cos(\Phi + \phi_2) |g_{-,2}(t_2)|^2 \right], \quad (2.19)$$

where Φ is a shorthand for $\omega - \phi_1 + \phi_2$. The $S_{n,1}(t_2)$ and $S_{h,1}(t_2)$ terms are induced by the interference between two oscillation paths $M_1^0 \rightarrow M_2^0 \rightarrow \bar{M}_2^0$ and $M_1^0 \rightarrow \bar{M}_1^0 \rightarrow \bar{M}_2^0$, as well as the interference between $M_1^0 \rightarrow M_2^0$ and $M_1^0 \rightarrow \bar{M}_1^0 \rightarrow \bar{M}_2^0 \rightarrow M_2^0$. The $S_{n,2}(t_2)$ and $S_{h,2}(t_2)$ terms are induced by the interference between $M_1^0 \rightarrow M_2^0$ and $M_1^0 \rightarrow \bar{M}_1^0 \rightarrow \bar{M}_2^0$ and also the interference between $M_1^0 \rightarrow M_2^0 \rightarrow \bar{M}_2^0$ and $M_1^0 \rightarrow \bar{M}_1^0 \rightarrow \bar{M}_2^0 \rightarrow M_2^0$. The other terms involved in (2.4) are

$$C_n(t_2) = \frac{e^{-\Gamma_2 t_2}}{2} \left\{ \sinh \frac{\Delta \Gamma_2 t_2}{2} \cos \phi_2 \left[\left| \frac{q_2}{p_2} \right| \left(1 + \left| \frac{p_1}{q_1} \right|^2 \right) - \left| \frac{p_2}{q_2} \right| \left(1 + \left| \frac{q_1}{p_1} \right|^2 \right) \right] \right. \\ \left. + \sin \Delta m_2 t_2 \sin \phi_2 \left[\left| \frac{q_2}{p_2} \right| \left(1 + \left| \frac{p_1}{q_1} \right|^2 \right) + \left| \frac{p_2}{q_2} \right| \left(1 + \left| \frac{q_1}{p_1} \right|^2 \right) \right] \right\} \\ + \frac{1}{2} \left[\left| \frac{q_2}{p_2} \right|^2 \left(1 + \left| \frac{p_1}{q_1} \right|^2 \right) - \left| \frac{p_2}{q_2} \right|^2 \left(1 + \left| \frac{q_1}{p_1} \right|^2 \right) \right] |g_{-,2}(t_2)|^2$$

$$-\frac{1}{2}\left(\left|\frac{q_1}{p_1}\right|^2 - \left|\frac{p_1}{q_1}\right|^2\right)|g_{+,2}(t_2)|^2, \quad (2.20)$$

$$\begin{aligned} C_h(t_2) = & \frac{e^{-\Gamma_2 t_2}}{2} \left\{ \sinh \frac{\Delta \Gamma_2 t_2}{2} \cos \phi_2 \left[\left| \frac{q_2}{p_2} \right| \left(1 - \left| \frac{p_1}{q_1} \right|^2 \right) - \left| \frac{p_2}{q_2} \right| \left(1 - \left| \frac{q_1}{p_1} \right|^2 \right) \right] \right. \\ & + \sin \Delta m_2 t_2 \sin \phi_2 \left[\left| \frac{q_2}{p_2} \right| \left(1 - \left| \frac{p_1}{q_1} \right|^2 \right) + \left| \frac{p_2}{q_2} \right| \left(1 - \left| \frac{q_1}{p_1} \right|^2 \right) \right] \Big\} \\ & + \frac{1}{2} \left[\left| \frac{q_2}{p_2} \right|^2 \left(1 - \left| \frac{p_1}{q_1} \right|^2 \right) - \left| \frac{p_2}{q_2} \right|^2 \left(1 - \left| \frac{q_1}{p_1} \right|^2 \right) \right] |g_{-,2}(t_2)|^2 \\ & + \frac{1}{2} \left(\left| \frac{q_1}{p_1} \right|^2 - \left| \frac{p_1}{q_1} \right|^2 \right) |g_{+,2}(t_2)|^2, \end{aligned} \quad (2.21)$$

$$\begin{aligned} S'_n(t_2) = & -\frac{1}{2} \left(\left| \frac{q_1}{p_1} \right| - \left| \frac{p_1}{q_1} \right| \right) \left\{ 2 \sin(\Phi - \phi_2) |g_{+,2}(t_2)|^2 + 2 \sin(\Phi + \phi_2) |g_{-,2}(t_2)|^2 \right. \\ & \left. + e^{-\Gamma_2 t_2} \left[\left(\left| \frac{q_2}{p_2} \right| + \left| \frac{p_2}{q_2} \right| \right) \sin \Phi \sinh \frac{\Delta \Gamma_2 t_2}{2} - \left(\left| \frac{q_2}{p_2} \right| - \left| \frac{p_2}{q_2} \right| \right) \cos \Phi \sin \Delta m_2 t_2 \right] \right\}, \end{aligned} \quad (2.22)$$

$$\begin{aligned} S'_h(t_2) = & \frac{1}{2} \left(\left| \frac{q_1}{p_1} \right| + \left| \frac{p_1}{q_1} \right| \right) \left\{ 2 \cos(\Phi - \phi_2) |g_{+,2}(t_2)|^2 + 2 \cos(\Phi + \phi_2) |g_{-,2}(t_2)|^2 \right. \\ & \left. + e^{-\Gamma_2 t_2} \left[\left(\left| \frac{q_2}{p_2} \right| + \left| \frac{p_2}{q_2} \right| \right) \cos \Phi \sinh \frac{\Delta \Gamma_2 t_2}{2} + \left(\left| \frac{q_2}{p_2} \right| - \left| \frac{p_2}{q_2} \right| \right) \sin \Phi \sin \Delta m_2 t_2 \right] \right\}, \end{aligned} \quad (2.23)$$

$$\begin{aligned} C'_n(t_2) = & \frac{e^{-\Gamma_2 t_2}}{2} \left\{ \sinh \frac{\Delta \Gamma_2 t_2}{2} \cos \phi_2 \left[\left| \frac{q_2}{p_2} \right| \left(1 - \left| \frac{p_1}{q_1} \right|^2 \right) + \left| \frac{p_2}{q_2} \right| \left(1 - \left| \frac{q_1}{p_1} \right|^2 \right) \right] \right. \\ & + \sin \Delta m_2 t_2 \sin \phi_2 \left[\left| \frac{q_2}{p_2} \right| \left(1 - \left| \frac{p_1}{q_1} \right|^2 \right) - \left| \frac{p_2}{q_2} \right| \left(1 - \left| \frac{q_1}{p_1} \right|^2 \right) \right] \Big\} \\ & + \frac{1}{2} \left[\left| \frac{q_2}{p_2} \right|^2 \left(1 - \left| \frac{p_1}{q_1} \right|^2 \right) + \left| \frac{p_2}{q_2} \right|^2 \left(1 - \left| \frac{q_1}{p_1} \right|^2 \right) \right] |g_{-,2}(t_2)|^2 \\ & - \frac{1}{2} \left(\left| \frac{q_1}{p_1} \right|^2 + \left| \frac{p_1}{q_1} \right|^2 - 2 \right) |g_{+,2}(t_2)|^2, \end{aligned} \quad (2.24)$$

$$\begin{aligned} C'_h(t_2) = & \frac{e^{-\Gamma_2 t_2}}{2} \left\{ \sinh \frac{\Delta \Gamma_2 t_2}{2} \cos \phi_2 \left[\left| \frac{q_2}{p_2} \right| \left(1 + \left| \frac{p_1}{q_1} \right|^2 \right) + \left| \frac{p_2}{q_2} \right| \left(1 + \left| \frac{q_1}{p_1} \right|^2 \right) \right] \right. \\ & + \sin \Delta m_2 t_2 \sin \phi_2 \left[\left| \frac{q_2}{p_2} \right| \left(1 + \left| \frac{p_1}{q_1} \right|^2 \right) - \left| \frac{p_2}{q_2} \right| \left(1 + \left| \frac{q_1}{p_1} \right|^2 \right) \right] \Big\} \\ & + \frac{1}{2} \left[\left| \frac{q_2}{p_2} \right|^2 \left(1 + \left| \frac{p_1}{q_1} \right|^2 \right) + \left| \frac{p_2}{q_2} \right|^2 \left(1 + \left| \frac{q_1}{p_1} \right|^2 \right) \right] |g_{-,2}(t_2)|^2 \\ & + \frac{1}{2} \left(\left| \frac{q_1}{p_1} \right|^2 + \left| \frac{p_1}{q_1} \right|^2 + 2 \right) |g_{+,2}(t_2)|^2. \end{aligned} \quad (2.25)$$

Again, if the decay occurs via $M_1^0 \rightarrow \bar{M}_2^0$ instead of $M_1^0 \rightarrow M_2^0$, the results can be directly obtained from (2.16) - (2.25) by replacing p_2/q_2 with q_2/p_2 .

Category 3

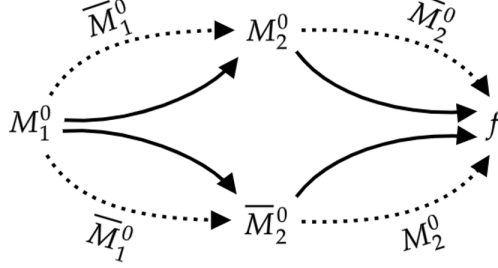


Figure 3. Eight oscillation paths in the cascade decay $M_1^0 \rightarrow M_2 \rightarrow f$, with $M_1^0 \rightarrow M_2^0, \bar{M}_2^0$, $\bar{M}_2^0 \rightarrow f, \bar{f}$ and their CP conjugate processes being allowed.

In the third category, M_1^0 can decay into both M_2^0 and \bar{M}_2^0 , so the number of possible paths for $M_1^0 \rightarrow M_2 \rightarrow f$ is doubled compared with the second category, as shown in **Figure 3**. To evaluate the CP asymmetry of such a process, the following parameters need to be introduced,

$$\frac{\langle M_2^0 | M_1^0 \rangle}{\langle \bar{M}_2^0 | M_1^0 \rangle} = r_1 e^{i(\delta_1 + \theta_1)}, \quad \frac{\langle f | \bar{M}_2^0 \rangle}{\langle f | M_2^0 \rangle} = r_2 e^{i(\delta_2 + \theta_2)}, \quad \frac{\langle M_2^0 | \bar{M}_1^0 \rangle}{\langle \bar{M}_2^0 | M_1^0 \rangle} = e^{i\theta_3}, \quad (2.26)$$

where $\delta_{1,2}$ are the relative strong phases, $\theta_{1,2,3}$ are the relative weak phases, and $r_{1,2}$ are the magnitude ratios. All complete results can be found in Appendix 1, where (A.3) and (A.5) correspond to the double-mixing CP violation terms. This is the most complex and comprehensive scenario, and by making appropriate approximations for this category, we can derive the complete results of the preceding two categories.

3 Numerical analysis

In this section, we will conduct numerical analyses of the double-mixing CP violation for various channels. As B_d^0 and B_s^0 have very different oscillation rates, we will discuss their decays separately. The input parameters involved are detailed in Table 1.

3.1 B_d^0 decays

In this subsection, we discuss the double-mixing CP violation in cascade B_d^0 decays. For the B_d^0 meson, it is a reasonable approximation to assume that the decay width difference, denoted as $\Delta\Gamma_{B_d}$, is negligible [38, 39]. Consequently, all terms involving $\sinh \Delta\Gamma_1 t_1/2$ in (2.4) can be disregarded while $\cosh \Delta\Gamma_1 t_1/2$ effectively equals 1. Furthermore, the magnitude of ratio q_{B_d}/p_{B_d} is approximated to be 1 [38, 39]. Under these approximations, the double-mixing CP violation A_{dm} is simplified to $A_{n,dm}$. Here, $A_{n,dm}$ represents the component of CP violation induced by double-mixing interference and it is proportional to

Parameter	Value	Parameter	Value
$ q_{B_d}/p_{B_d} $	1.0010 ± 0.0008 [39]	x_{B_d}	0.769 ± 0.004 [38]
$ q_{B_s}/p_{B_s} $	1.0003 ± 0.0014 [39]	x_{B_s}	27.03 ± 0.09 [38]
$ q_K/p_K $	0.996774 ± 0.000019 [38]	x_K	0.946 ± 0.002 [38]
$ q_D/p_D $	0.995 ± 0.016 [39]	x_D	$(4.1 \pm 0.5) \times 10^{-3}$ [39]
ϕ_{B_d}	$(44.4 \pm 1.4)^\circ$ [38]	y_{B_d}	-0.0005 ± 0.0050 [38]
ϕ_{B_s}	$-(2.106 \pm 0.135)^\circ$ [38]	y_{B_s}	-0.064 ± 0.003 [38]
ϕ_K	$(0.176 \pm 0.001)^\circ$ [38]	y_K	-0.996506 ± 0.000016 [38]
ϕ_D	$-(177.5 \pm 1.2)^\circ$ [38]	y_D	$(6.2 \pm 0.6) \times 10^{-3}$ [39]
ω_{B_d}	$(0.00372^{+0.00025}_{-0.00023})^\circ$ [38]	ω_{B_s}	$(-0.070^{+0.004}_{-0.005})^\circ$ [38]
ω_K	$(43.52 \pm 0.05)^\circ$ [38]	ω_D	$(83.4446^{+32.2995}_{-36.5375})^\circ$ [38]
ω_1	0° [38]	ω_2	$(65.54 \pm 1.55)^\circ$ [38]
ω_3	0° [38]	ω_4	$(-114.419 \pm 1.549)^\circ$ [38]
r_D	$-(5.857 \pm 0.017) \times 10^{-2}$ [39]	δ_D	$(7.2^{+7.9}_{-9.2})^\circ$ [39]

Table 1. The input parameters and their values, with $x_M \equiv \Delta m_M/\Gamma_M$ and $y_M \equiv \Delta\Gamma_M/(2\Gamma_M)$, respectively.

$\sin \Delta m_1 t_1$. This simplification aids in a more straightforward analysis of the double-mixing CP violation effect in B_d^0 decays.

3.1.1 $B_d^0 \rightarrow J/\psi K \rightarrow J/\psi(\pi^\pm \ell^\mp \nu)$

We initially explore the decay channel $B_d^0 \rightarrow J/\psi K \rightarrow J/\psi(\pi^+ \ell^- \bar{\nu}_\ell)$. The decay mode $B_d^0 \rightarrow J/\psi K^0$, corresponding to the $b \rightarrow c\bar{c}s$ transition at the quark level, is frequently employed for the extraction of the CKM angle β because of the tiny pollution of strong interaction and the relatively substantial CP violation effect [38]. The cascading mixing effect in this decay channel where the secondary decay is semileptonic has been previously investigated in paper [40].

In this decay channel, only the paths $B_d^0 \rightarrow J/\psi K^0 \rightarrow J/\psi \bar{K}^0 \rightarrow J/\psi(\pi^+ \ell^- \bar{\nu}_\ell)$ and $B_d^0 \rightarrow \bar{B}_d^0 \rightarrow J/\psi \bar{K}^0 \rightarrow J/\psi(\pi^+ \ell^- \bar{\nu}_\ell)$ can contribute. This case aligns with the first category defined previously. As a reasonable approximation, we have neglected the direct CP violation in neutral K meson decay, assuming $\langle \pi^+ \ell^- \bar{\nu}_\ell | \bar{K}^0 \rangle = \langle \pi^- \ell^+ \nu_\ell | K^0 \rangle$. The primary decay amplitudes are related as $\langle J/\psi \bar{K}^0 | \bar{B}_d^0 \rangle = -\langle J/\psi K^0 | B_d^0 \rangle e^{i\omega_{B_d}}$, where ω_{B_d} is a pure weak phase, with the latest result given by $\arg(V_{cb}V_{cs}^*/V_{cb}^*V_{cs}) = (0.00372^{+0.00025}_{-0.00023})^\circ$ [38]. It is important to note that, the minus sign originates from the convention $CP |J/\psi K^0\rangle = -|J/\psi \bar{K}^0\rangle$. Then, all the components in (2.4) are calculated as:

$$\begin{aligned}
A_{n,dm}(t_1, t_2) = \frac{e^{-(\Gamma_{B_d} t_1 + \Gamma_K t_2)}}{2D(t_1, t_2)} & \left\{ \sinh \frac{\Delta\Gamma_K t_2}{2} \sin \Phi_1 \left(\left| \frac{p_K}{q_K} \right| + \left| \frac{q_K}{p_K} \right| \right) \right. \\
& \left. - \sin \Delta m_K t_2 \cos \Phi_1 \left(\left| \frac{q_K}{p_K} \right| - \left| \frac{p_K}{q_K} \right| \right) \right\} \sin \Delta m_{B_d} t_1, \quad (3.1)
\end{aligned}$$

t_1/τ_{B_d}	t_2/τ_K	A_{CP}
0~3	0~ 2	40.52%
0~2	0~ 2	39.76%
0~3	0~ 1	42.09%
0~2	0~ 1	48.04%
0~3	0~ 0.5	29.28%
0~2	0~ 0.5	38.76%

Table 2. The time integrated A_{CP} in $B_d^0 \rightarrow J/\psi K \rightarrow J/\psi(\pi^+\ell^-\bar{\nu}_\ell)$.

$$A_{non-dm}(t_1, t_2) = \frac{1}{D(t_1, t_2)} \left(\left| \frac{q_K}{p_K} \right|^2 - \left| \frac{p_K}{q_K} \right|^2 \right) |g_{-,K}(t_2)|^2 |g_{+,B_d}(t_1)|^2, \quad (3.2)$$

where Φ_1 is defined as $\omega_{B_d} - \phi_{B_d} + \phi_K$, approximated as -2β . The denominator $D(t_1, t_2)$ is given by (2.4) with the t_2 functions substituted with (2.11) - (2.13). Hence, by measuring the double-mixing CP violation of this channel, the β angle can be extracted. The double-mixing CP violation $A_{n,dm}(t_1, t_2)$ is induced by the interference between the decay paths $B_d^0 \rightarrow J/\psi K^0 \rightarrow J/\psi \bar{K}^0 \rightarrow J/\psi(\pi^+\ell^-\bar{\nu}_\ell)$ and $B_d^0 \rightarrow \bar{B}_d^0 \rightarrow J/\psi \bar{K}^0 \rightarrow J/\psi(\pi^+\ell^-\bar{\nu}_\ell)$, corresponding to the $S_n(t_2)$ component in (2.4). Meanwhile, $A_{non-dm}(t_1, t_2)$ corresponds to the $C_+(t_2)$ term within $N(t_1, t_2)$ as defined in (2.4).

To investigate the double-mixing CP violation effect, we conducted a numerical analysis of both the total CP asymmetry A_{CP} and the double-mixing CP asymmetry A_{dm} . Notably, A_{dm} plays a crucial role in A_{CP} , as evidenced by the mathematical formula in (3.1) and the corresponding numerical results in **Figure 4**. The left panel clearly shows that the maximum value of the two-dimensional time-dependent double-mixing CP asymmetry can even exceed 50%. When integrating t_2 from 0 to $2\tau_K$, as depicted in the middle panel, the double-mixing effect almost overlaps with the total CP asymmetry A_{CP} , indicating its dominance. Its magnitude initially increases with t_1 and then decreases, a pattern attributed to its sine dependence on t_1 . Within an interval of $4\tau_{B_d}$, it completes only half an oscillation period, consistent with the small value of x_{B_d} listed in Table 1. Similar trends are observed when considering the dependence on t_2 , as shown in the right panel, where t_1 is integrated from 0 to $3\tau_{B_d}$. It rapidly increases within a period shorter than τ_K , and then decreases before stabilizing. This phenomenon can be explained by the fact that the numerator is mainly dominated by the first term in (3.1), which increases from 0 to τ_K and then stabilizes. and that the denominator is dominated by $C'_+(t_2)$ and $C'_-(t_2)$, which decreases from 0 to $0.5\tau_K$ and then steadily increases until around $t_2 \approx 2.5\tau_K$. A comprehensive two-dimensional time integration of $A_{CP}(t_1, t_2)$ yields the results presented in Table 2. For experimental convenience, we perform the integration over different t_1 and t_2 intervals. The integrated A_{CP} fluctuates around 30-40% with different configurations.

The yield of $B_d^0 \rightarrow J/\psi K_S^0$ has been previously observed at LHCb [41] using data from Run 1 of the LHC at a center-of-mass energy $\sqrt{s} = 7$ TeV with an integrated luminosity 3 fb⁻¹. This observation involved the final states of $J/\psi \rightarrow \mu^+\mu^-$ and $K_S^0 \rightarrow \pi^+\pi^-$. Based

on this study, we estimate the yield of $B_d^0 \rightarrow J/\psi K \rightarrow J/\psi(\pi^+\ell^-\bar{\nu}_\ell)$ with 300 fb^{-1} to be approximately 3.6×10^4 .

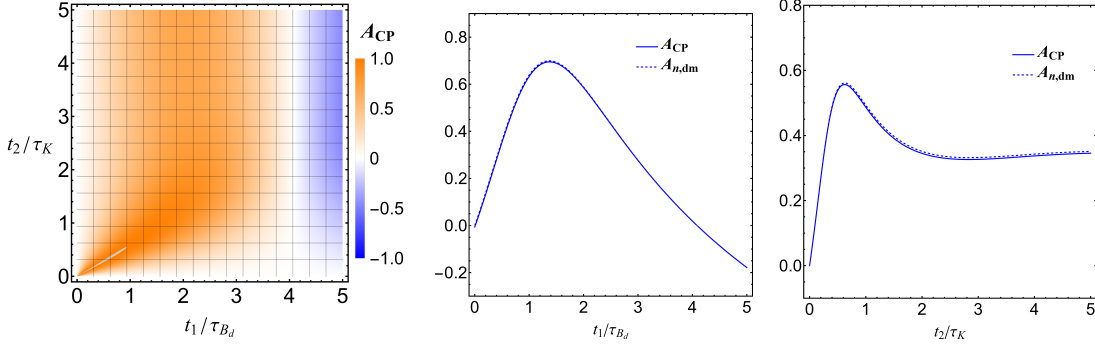


Figure 4. Time dependence of the double-mixing CP asymmetry A_{CP} in $B_d^0(t_1) \rightarrow J/\psi K(t_2) \rightarrow J/\psi(\pi^+\ell^-\bar{\nu}_\ell)$. The left panel displays the two-dimensional time dependence. The middle panel and the right panel display the dependence on t_1 (with t_2 integrated from 0 to $2\tau_K$) and t_2 (with t_1 integrated from 0 to $3\tau_{B_d}$), respectively.

Substituting the semileptonic final state with $\pi^-\ell^+\nu_\ell$ instead of $\pi^+\ell^-\bar{\nu}_\ell$ resulting in two viable decay paths, denoted as $B_d^0 \rightarrow J/\psi K^0 \rightarrow J/\psi(\pi^-\ell^+\nu_\ell)$ and $B_d^0 \rightarrow \bar{B}_d^0 \rightarrow J/\psi \bar{K}^0 \rightarrow J/\psi K^0 \rightarrow J/\psi(\pi^-\ell^+\nu_\ell)$. The corresponding CP asymmetries are then calculated to be

$$A_{n,dm}(t_1, t_2) = \frac{e^{-(\Gamma_{B_d}t_1 + \Gamma_K t_2)}}{2D(t_1, t_2)} \left\{ \sinh \frac{\Delta\Gamma_K t_2}{2} \sin \Phi_1 \left(\left| \frac{p_K}{q_K} \right| + \left| \frac{q_K}{p_K} \right| \right) - \sin \Delta m_K t_2 \cos \Phi_1 \right. \\ \left. \times \left(\left| \frac{q_K}{p_K} \right| - \left| \frac{p_K}{q_K} \right| \right) \right\} \sin \Delta m_{B_d} t_1, \quad (3.3)$$

$$A_{non-dm}(t_1, t_2) = \frac{1}{D(t_1, t_2)} \left(-\left| \frac{q_K}{p_K} \right|^2 + \left| \frac{p_K}{q_K} \right|^2 \right) |g_{-,K}(t_2)|^2 |g_{-,B_d}(t_1)|^2. \quad (3.4)$$

The denominator $D(t_1, t_2)$ here can be obtained by combining (2.4) with (2.11) - (2.13), while also performing the substitution $C'_+(t_2) \leftrightarrow C'_-(t_2)$, and adding an extra negative sign in front of $S'_n(t_2)$.

Compared to the final state $\pi^+\ell^-\bar{\nu}_\ell$, a key difference for the final state $\pi^-\ell^+\nu_\ell$ lies in an additional negative sign in the numerator of the non-double-mixing CP violation term $A_{non-dm}(t_1, t_2)$, as illustrated in **Figure 5**. The double-mixing CP violation remains significant, with the peak occurring later compared to the decay process with the final state $\pi^+\ell^-\bar{\nu}_\ell$. For instance, the peak in the middle panel of **Figure 5** occurs at around $t_1 = 3\tau_{B_d}$, in contrast to about $1.5\tau_{B_d}$ for the other final state. This difference is due to an additional negative sign in the term $S'_n(t_2)$ in (2.4). Moreover, the magnitude of CP violation increases significantly over time, reflecting the later occurrence of its peak in both t_1 and t_2 .

3.1.2 $B_d^0 \rightarrow J/\psi K \rightarrow J/\psi f_+$

We now analyze the double-mixing CP violation in the decay chain $B_d^0 \rightarrow J/\psi K \rightarrow J/\psi f_+$. In this context, f_+ refers to CP-even final states, such as $\pi^+\pi^-$. Notably, the CP-even state under consideration is common to K^0 and \bar{K}^0 . This will lead to four conceivable

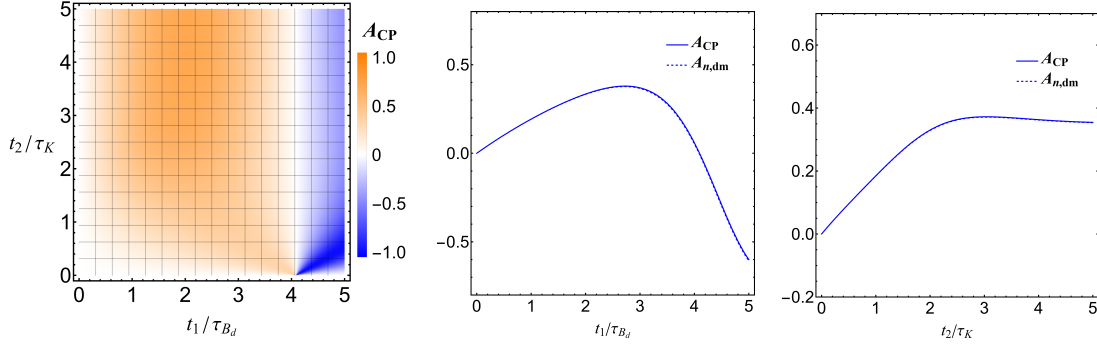


Figure 5. Time dependence of the double-mixing CP asymmetry A_{CP} in $B_d^0(t_1) \rightarrow J/\psi K(t_2) \rightarrow J/\psi(\pi^- \ell^+ \nu_\ell)$. The left panel displays the two-dimensional time dependence. The middle panel and the right panel display the dependence on t_1 (with t_2 integrated from 0 to $2\tau_K$) and t_2 (with t_1 integrated from 0 to $3\tau_{B_d}$), respectively.

decay paths: $B_d^0 \rightarrow K^0 \rightarrow f_+$, $B_d^0 \rightarrow K^0 \rightarrow \bar{K}^0 \rightarrow f_+$, $B_d^0 \rightarrow \bar{B}_d^0 \rightarrow \bar{K}^0 \rightarrow f_+$ and $B_d^0 \rightarrow \bar{B}_d^0 \rightarrow \bar{K}^0 \rightarrow K^0 \rightarrow f_+$. Hence, it belongs to the second category in our classification. Considering the negligible direct CP violation in the neutral K meson ($\langle f_+ | K^0 \rangle = \langle f_+ | \bar{K}^0 \rangle$) and the suppressed penguin amplitudes in $B_d^0 \rightarrow J/\psi K^0$ (both Cabbibo-suppressed and loop-suppressed as indicated in [38]), we obtain all components of the two-dimensional time-dependent CP asymmetry $A_{CP}(t_1, t_2)$ in (2.4) as follows:

$$A_{n,dm}(t_1, t_2) = \frac{e^{-(\Gamma_{B_d} t_1 + \Gamma_K t_2)}}{D(t_1, t_2)} \left\{ \sin \Delta m_K t_2 \left(\left| \frac{q_K}{p_K} \right| - \left| \frac{p_K}{q_K} \right| \right) \cos \Phi_1 - \sinh \frac{\Delta \Gamma_K t_2}{2} \left(\left| \frac{q_K}{p_K} \right| + \left| \frac{p_K}{q_K} \right| \right) \sin \Phi_1 \right\} \sin \Delta m_{B_d} t_1, \quad (3.5)$$

$$A_{non-dm}(t_1, t_2) = \frac{2e^{-\Gamma_{B_d} t_1}}{D(t_1, t_2)} \left\{ \sin(\phi_{B_d} - \omega_{B_d}) |g_{+,K}(t_2)|^2 + \sin(\phi_{B_d} - \omega_{B_d} + 2\phi_K) |g_{-,K}(t_2)|^2 \right\} \sin \Delta m_{B_d} t_1. \quad (3.6)$$

In this situation, $A_{n,dm}$ and A_{non-dm} constitute S_n in (2.4). Notably, $\Phi_1 \approx -2\beta$, $\phi_{B_d} - \omega_{B_d} \approx 2\beta$ and $\phi_K \approx 0$. Under the approximation that $|q_K/p_K| \approx 1$, $S_n(t_2)$ simplifies to

$$S_n(t_2) = 2 \sin 2\beta e^{-\Gamma_S t_2}. \quad (3.7)$$

By taking $q_K/p_K \rightarrow 1$, we neglect the indirect CP violation of neutral kaon, so only $K_S^0 \rightarrow f_+$ contributes to the decay and it explains why only the $e^{-\Gamma_S t_2}$ term survives. As a result, the total CP asymmetry A_{CP} is expressed as

$$A_{CP}(t_1, t_2) = \sin 2\beta \cdot \sin \Delta m_{B_d} t_1, \quad (3.8)$$

which is consistent with the formulas (13.74) and (13.82) in the “CP Violation in the Quark Sector” review of the PDG [38].

We conducted a numerical analysis of A_{CP} and A_{dm} for this process. The two-dimensional time-dependent CP violation result is shown in the left panel of **Figure 6**,

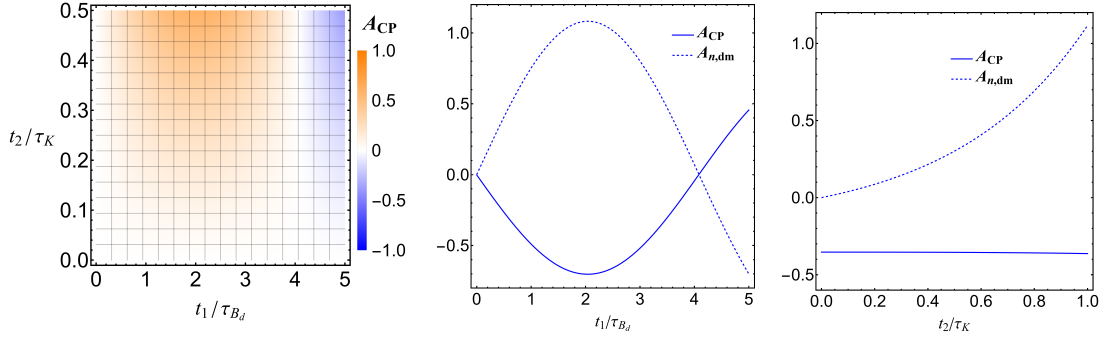


Figure 6. Time dependence of the CP asymmetry A_{CP} in $B_d^0(t_1) \rightarrow J/\psi K(t_2) \rightarrow J/\psi(\pi^+\pi^-)$. The left panel displays the two-dimensional time dependence. The middle panel and the right panel display the dependence on t_1 (with t_2 integrated from 0 to $2\tau_K$) and t_2 (with t_1 integrated from 0 to $3\tau_{B_d}$), respectively.

t_1/τ_{B_d}	t_2/τ_K	A_{CP}
0~3	0~2	-35.36%
0~2	0~2	-32.35%
0~3	0~1	-35.30%
0~2	0~1	-32.28%
0~3	0~0.5	-35.31%
0~2	0~0.5	-32.27%

Table 3. Time integrated A_{CP} in $B_d^0 \rightarrow J/\psi K \rightarrow J/\psi(\pi^+\pi^-)$.

with its peak appearing around $t_1 = 2\tau_{B_d}$ and $t_2 > 0.5\tau_K$. By integrating t_2 from 0 to $2\tau_K$, the t_1 -dependent result, displayed in the middle panel, reaches its peak at $t_1 = 2\tau_{B_d}$. Since both A_{CP} and $A_{n,dm}$ exhibit sine dependence on t_1 , their oscillations are similar, but with different magnitudes and signs. It can be concluded that the double-mixing contribution and the non-double-mixing contribution have opposite signs, with the former having a smaller magnitude. The right panel of **Figure 6** shows that A_{CP} with t_1 integrated out is almost independent of t_2 . On the other hand, the $A_{n,dm}$ part, with its hyperbolic sine dependence on t_2 , increases with t_2 ranging from 0 to τ_K . The two-dimensional time integration of $A_{\text{CP}}(t_1, t_2)$ for this channel is given in Table 3, demonstrating its insensitivity to changes in both t_1 and t_2 , owing to the fact that most of the decays occur earlier.

3.1.3 $B_d^0 \rightarrow DK \rightarrow (K^-\pi^+)(\pi^+\ell^-\bar{\nu}_\ell)$

The decay $B_d^0 \rightarrow DK^*$ is well-known for its precision in measuring the angle γ . First attempts to constraint γ using $B_d^0 \rightarrow DK^*$ decays have adopted neutral D meson decays into $K_S^0\pi^+\pi^-$ [42] and suppressed final states such as $K^-\pi^+$, with relevant branching ratio and parameters measured in several studies [43–45]. Here, we consider a similar process $B_d^0 \rightarrow DK$, which was also briefly discussed in our previous work [37]. This channel, comprising two oscillating paths, $B_d^0 \rightarrow D^0 K^0 \rightarrow D^0 \bar{K}^0$ and $B_d^0 \rightarrow \bar{B}_d^0 \rightarrow D^0 \bar{K}^0$, falls within the first

t_1/τ_{B_d}	t_2/τ_K	A_{CP}
0~3	0~ 2	26.36%
0~2	0~ 2	31.28%
0~3	0~ 1	15.68%
0~2	0~ 1	19.79%
0~3	0~ 0.5	8.78%
0~2	0~ 0.5	11.52%

Table 4. Time integrated A_{CP} in $B_d^0 \rightarrow DK \rightarrow (K^- \pi^+)(\pi^+ \ell^- \bar{\nu}_\ell)$.

category. The following relations are employed to evaluate the CP asymmetry,

$$\frac{A(\bar{B}_d^0 \rightarrow D^0 \bar{K}^0)}{A(B_d^0 \rightarrow \bar{D}^0 K^0)} = e^{i\omega_1}, \quad \omega_1 = \arg \frac{V_{cb}^* V_{us}^*}{V_{cb}^* V_{us}}, \quad (3.9)$$

$$\frac{A(\bar{B}_d^0 \rightarrow D^0 K^0)}{A(B_d^0 \rightarrow \bar{D}^0 K^0)} = r_B e^{i(\delta_B + \omega_2)}, \quad \omega_2 = \arg \frac{V_{ub}^* V_{cs}^*}{V_{cb}^* V_{us}}, \quad (3.10)$$

where r_B and δ_B are the magnitudes and the strong phase of the ratio, respectively. The parameters for the decay channel $B_d^0 \rightarrow DK^*$ have been determined by the LHCb experiment [46, 47], and we take similar values for $B_d^0 \rightarrow DK$: $r_B = 0.366$ and $\delta_B = 164^\circ$. We neglect the direct CP violation in neutral K meson decay, *i.e.*, $\langle f | \bar{K}^0 \rangle = \langle \bar{f} | K^0 \rangle$, as well as the amplitude of Cabibbo-suppressed process $\bar{D}^0 \rightarrow K^- \pi^+$ and the mixing of the neutral D meson. The double-mixing term is

$$A_{n,dm}(t_1, t_2) = \frac{e^{-\Gamma_{B_d} t_1}}{D(t_1, t_2)} S_n(t_2) \sin \Delta m_{B_d} t_1, \quad (3.11)$$

$$S_n(t_2) = e^{-\Gamma_K t_2} r_B \left\{ \left| \frac{q_K}{p_K} \right| \left[\sin(\delta_B + \delta_\omega) \sinh \frac{1}{2} \Delta \Gamma_K t_2 + \cos(\delta_B + \delta_\omega) \sin \Delta m_K t_2 \right] \right. \\ \left. - \left| \frac{p_K}{q_K} \right| \left[\sin(\delta_B - \delta_\omega) \sinh \frac{1}{2} \Delta \Gamma_K t_2 + \cos(\delta_B - \delta_\omega) \sin \Delta m_K t_2 \right] \right\}, \quad (3.12)$$

where $\delta_\omega = \omega_2 - \omega_1 + \phi_{B_d} - \phi_K$, approximating $2\beta + \gamma$. Applying (2.11) - (2.13) yields the result of $D(t_1, t_2)$, with $C'_+(t_2)$ has an additional factor of r_B^2 , and $S'_n(t_2)$ can be obtained by changing the negative sign in front of $|p_K/q_K|$ in (3.12) to a positive sign.

Our numerical analysis addresses both the total CP asymmetry A_{CP} and the double-mixing CP asymmetry A_{dm} . As illustrated in the left panel of **Figure 7**, the maximum value of two-dimensional time-dependent double-mixing results can surpass 50% when t_1 is small. From the t_1 and t_2 dependence displayed in the middle and right panels, respectively, it can be seen that the double-mixing effect dominates. This trend resembles that observed in $B_d^0 \rightarrow J/\psi K \rightarrow J/\psi(\pi^+ \ell^- \bar{\nu}_\ell)$, albeit with differences attributed to the suppression factor r_B and a negative sign in δ_ω . With integrating t_1 from 0 to $3\tau_{B_d}$, a steady growth of A_{CP} with respect to t_2 is observed. This is supported by the time-integrated A_{CP} presented in **Table 4**, which shows sensitivity to changes in the upper limit of t_2 .

Given that the weak phase involved in this decay $\delta_\omega \approx 2\beta + \gamma$, its extraction holds significant importance. It should be emphasized that the weak phase can be directly extracted from experimental data, as discussed in our previous study [37].

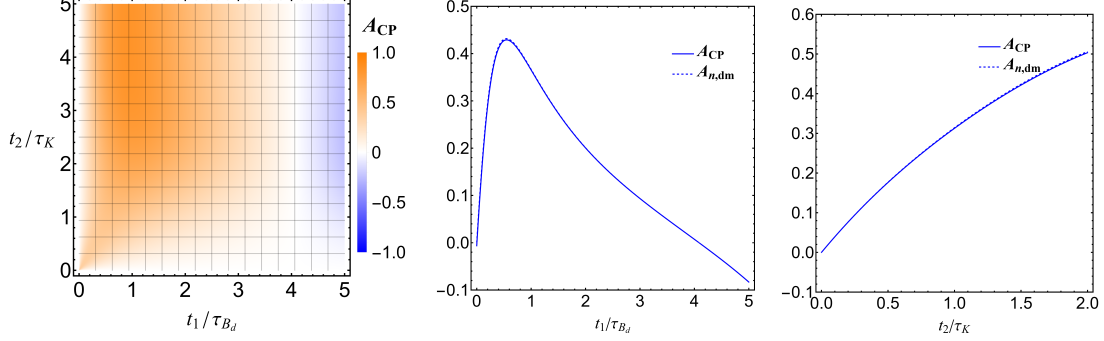


Figure 7. Time dependence of the double-mixing CP asymmetry A_{CP} in $B_d^0(t_1) \rightarrow DK(t_2) \rightarrow (K^-\pi^+)(\pi^+\ell^-\bar{\nu}_\ell)$. The left panel displays the two-dimensional time dependence. The middle panel and the right panel display the dependence on t_1 (with t_2 integrated from 0 to $2\tau_K$) and t_2 (with t_1 integrated from 0 to $3\tau_{B_d}$), respectively.

3.1.4 $B_d^0 \rightarrow DK_S^0 \rightarrow f_+ K_S^0$

Distinct from $B_d^0 \rightarrow DK \rightarrow (K^-\pi^+)(\pi^+\ell^-\bar{\nu}_\ell)$ discussed previously in section 3.1.3, when considering the CP-even final state like $f_+ = \pi^+\pi^-$ of D in $B_d^0 \rightarrow DK_S^0 \rightarrow f_+ K_S^0$, both intermediate D^0 and \bar{D}^0 contributions are comparable. With primary $b \rightarrow u$ and $b \rightarrow c$ transitions, both B_d^0 and \bar{B}_d^0 can decay into states involving either D^0 or \bar{D}^0 . These make this channel a particularly intricate case, categorizing it within the third classification.

The terms related to the double-mixing CP violation are expressed as below:

$$\begin{aligned}
A_{n,dm,1}(t_1, t_2) = & f(t_1, t_2) e^{-\Gamma_D t_2} \sinh \frac{1}{2} \Delta \Gamma_D t_2 \left\{ - \left(\left| \frac{p_D}{q_D} \right| + \left| \frac{q_D}{p_D} \right| \right) \sin(\omega_1 - \phi_{B_d} - \phi_D) \right. \\
& - r_B \left[\left| \frac{p_D}{q_D} \right| \sin(\delta_B + \Phi_2) - \left| \frac{q_D}{p_D} \right| \sin(\delta_B - \Phi_2) \right. \\
& + \left. \left| \frac{p_D}{q_D} \right| \sin(\delta_B + \Phi_3) - \left| \frac{q_D}{p_D} \right| \sin(\delta_B - \Phi_3) \right] \\
& \left. - r_B^2 \left(\left| \frac{p_D}{q_D} \right| + \left| \frac{q_D}{p_D} \right| \right) \sin(\Phi_2 - \omega_2) \right\}, \tag{3.13}
\end{aligned}$$

$$\begin{aligned}
A_{n,dm,2}(t_1, t_2) = & f(t_1, t_2) e^{-\Gamma_D t_2} \sin \Delta m_D t_2 \left\{ \left(\left| \frac{p_D}{q_D} \right| - \left| \frac{q_D}{p_D} \right| \right) \cos(\omega_1 - \phi_{B_d} - \phi_D) \right. \\
& - r_B \left[\left| \frac{p_D}{q_D} \right| \cos(\delta_B + \Phi_2) - \left| \frac{q_D}{p_D} \right| \cos(\delta_B - \Phi_2) \right. \\
& - \left. \left| \frac{p_D}{q_D} \right| \cos(\delta_B + \Phi_3) + \left| \frac{q_D}{p_D} \right| \cos(\delta_B - \Phi_3) \right] \\
& \left. - r_B^2 \left(\left| \frac{p_D}{q_D} \right| - \left| \frac{q_D}{p_D} \right| \right) \cos(\Phi_2 - \omega_2) \right\}, \tag{3.14}
\end{aligned}$$

where $\Phi_2 = \omega_1 - \omega_2 - \phi_{B_d} + \phi_D$, $\Phi_3 = \omega_1 - \omega_2 - \phi_{B_d} - \phi_D$ and $f(t_1, t_2) = e^{-\Gamma_{B_d} t_1} \sin \Delta m_{B_d} t_1 / D(t_1, t_2)$, and the double-mixing CP violation is the sum of these two contributions. Combining (2.4) and (2.22) - (2.25) yields the denominator $D(t_1, t_2)$. The parameters r_B and δ_B have been defined in (3.9).

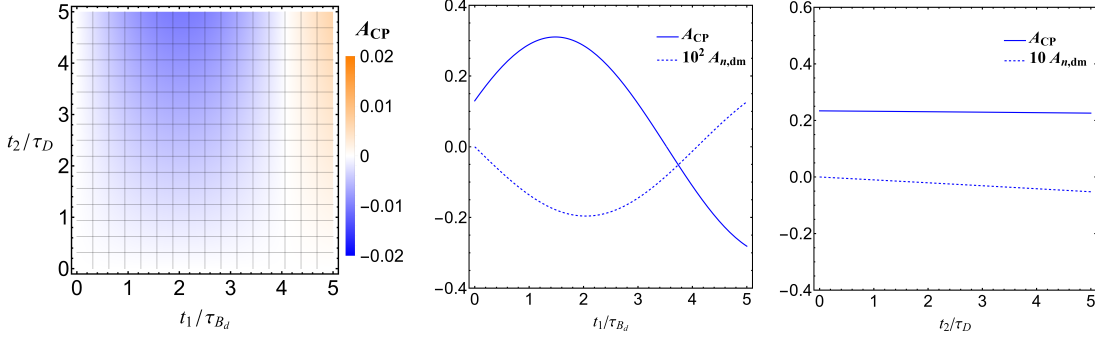


Figure 8. Time dependence of the CP asymmetry A_{CP} in $B_d^0(t_1) \rightarrow D(t_2)K_S^0 \rightarrow (\pi^+\pi^-)K_S^0$. The left panel displays the two-dimensional time dependence. The middle panel and the right panel display the dependence on t_1 (with t_2 integrated from 0 to $5\tau_D$) and t_2 (with t_1 integrated from 0 to $3\tau_{B_d}$), respectively.

We perform the numerical analysis assuming the parameter values $r_B = 0.366$ and $\delta_B = 164^\circ$ as in section 3.1.3. The results are depicted in **Figure 8**. On the left panel, the two-dimensional time-dependent CP violation exhibits a distribution akin to the decay channel $B_d^0 \rightarrow J/\psi K \rightarrow J/\psi(\pi^+\pi^-)$, but with peak values significantly lower. Integrating t_2 from 0 to $5\tau_D$, we present the t_1 -dependent results in the middle panel, revealing tiny double-mixing CP violation. This is primarily attributed to the small magnitudes of x_D and y_D , both approximately 10^{-3} . These small values reduces both $\sinh \frac{1}{2}\Delta\Gamma_D t_2$ and $\sin \Delta m_D t_2$. The right panel of **Figure 8** shows the t_2 dependence of A_{CP} when integrating t_1 from 0 to $3\tau_{B_d}$. The near-linear dependency of A_{dm} on t_2 is primarily due to its denominator being dominated by the $\cosh y_D t_2$ term and its numerator by the $\sinh x_D t_2$ term. It is concluded that the CP asymmetry in this channel is dominated by the part induced by the interference between the $b \rightarrow c$ and $b \rightarrow u$ amplitudes, and the part induced by the interference between decays with and without B mixing, while the double-mixing CP violation is negligible owing to tiny D -mixing effect.

3.1.5 $B_d^0 \rightarrow DK_S^0 \rightarrow (K^-\pi^+)K_S^0$

The last B_d^0 decay channel selected is $B_d^0 \rightarrow DK_S^0 \rightarrow (K^-\pi^+)K_S^0$. The observation of a similar channel $\bar{B}_d^0 \rightarrow D^0 \bar{K}^{*0}$ was reported by [43, 44], but the branching ratio and relevant parameters were measured using self-tagging methods and thus the mixing effect was not considered. In this channel, the intermediate D meson can be either D^0 or \bar{D}^0 , although the latter has a suppressed contribution. Therefore, this channel is categorized as the third type.

To present the result of the CP asymmetry, we introduce the amplitude ratio of the

t_1/τ_{B_d}	t_2/τ_D	A_{CP}
0~3	0~5	-60.71%
0~2	0~5	-69.20%
0~3	0~4	-60.71%
0~2	0~4	-69.20%

Table 5. Two-dimensional time integration of $A_{CP}(t_1, t_2)$ in $B_d^0(t_1) \rightarrow D(t_2)K_S^0 \rightarrow (K^-\pi^+)K_S^0$.

primary decay as in (3.9) and the ratio of the secondary decay as

$$\frac{A(\bar{D}^0 \rightarrow K^-\pi^+)}{A(D^0 \rightarrow K^-\pi^+)} = -r_D e^{-i\delta_D}, \quad (3.15)$$

where the numerical values for magnitude ratio r_D and the strong phase δ_D are listed in Table 1. The direct CP violation in the D meson decays is neglected due to the minimal weak phases between the first two generations of quarks. The double-mixing term in (2.4) is expressed as

$$A_{n,dm}(t_1, t_2) = -\frac{e^{-(\Gamma_{B_d}t_1 + \Gamma_D t_2)}}{2D(t_1, t_2)} \left[\left(\left| \frac{q_D}{p_D} \right| + \left| \frac{p_D}{q_D} \right| \right) \sin(\omega_1 - \phi_{B_d} - \phi_D) \sinh \frac{1}{2} \Delta \Gamma_D t_2 \right. \\ \left. + \left(\left| \frac{q_D}{p_D} \right| - \left| \frac{p_D}{q_D} \right| \right) \cos(\omega_1 - \phi_{B_d} - \phi_D) \sin \Delta m_D t_2 \right] \sin \Delta m_{B_d} t_1, \quad (3.16)$$

where the contributions below $\mathcal{O}(10^{-3})$ have been neglected. It turns out that the corrections from the doubly Cabibbo-suppressed $D^0 \rightarrow K^+\pi^-$ decay are negligible, so practically only the interference term between $B_d^0 \rightarrow \bar{D}^0 \rightarrow D^0$ and $B_d^0 \rightarrow \bar{B}_d^0 \rightarrow D^0$ is retained. With also the contributions below $\mathcal{O}(10^{-3})$ neglected, the non-double-mixing CP asymmetry reads

$$A_{non-dm,1}(t_1, t_2) = r_B \left\{ \left(\left| \frac{p_D}{q_D} \right| \cos(\delta_B + \omega_2 - \phi_D) - \left| \frac{q_D}{p_D} \right| \cos(\delta_B - \omega_2 + \phi_D) \right) \sinh \frac{1}{2} \Delta \Gamma_D t_2 \right. \\ \left. + \left(\left| \frac{p_D}{q_D} \right| \sin(\delta_B + \omega_2 - \phi_D) - \left| \frac{q_D}{p_D} \right| \sin(\delta_B - \omega_2 + \phi_D) \right) \sin \Delta m_D t_2 \right. \\ \left. + 2r_D \sin(\delta_B - \delta_D) \sin \omega_2 \left(\cosh \frac{1}{2} \Delta \Gamma_D t_2 + \cos \Delta m_D t_2 \right) \right\} f(t_1, t_2), \\ A_{non-dm,2}(t_1, t_2) = -2 \frac{e^{-\Gamma_{B_d} t_1}}{D(t_1, t_2)} \left\{ r_B \cos \delta_B \sin(\omega_1 - \omega_2 - \phi_{B_d}) + r_D \cos \delta_D \sin(\omega_1 - \phi_{B_d}) \right\} \\ \times |g_{+,D}(t_2)|^2 \sin \Delta m_{B_d} t_1, \quad (3.17)$$

where $f(t_1, t_2) \equiv e^{-\Gamma_D t_2} |g_{+,B_d}(t_1)|^2 / 4D(t_1, t_2)$. The denominator $D(t_1, t_2)$ can be derived by combining (2.4) with (A.7) - (A.12), while maintaining consistency with all the approximations used in the numerator. The parameters r_B and δ_B have been defined in (3.9). The non-double-mixing CP asymmetry contains r_D in the expression (3.17), indicating that the doubly Cabibbo-suppressed $D^0 \rightarrow K^+\pi^-$ contribution is considerable here.

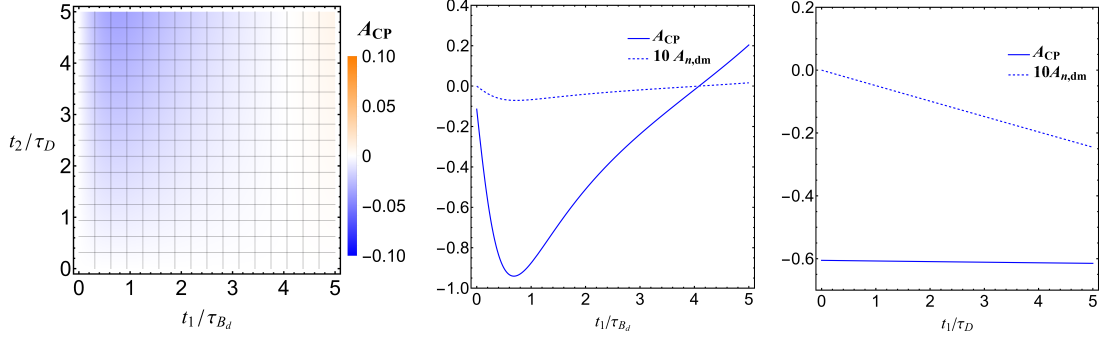


Figure 9. Time dependence of the CP asymmetry A_{CP} in $B_d^0(t_1) \rightarrow D(t_2)K_S^0 \rightarrow (K^-\pi^+)K_S^0$. The left panel displays the two-dimensional time dependence. The middle panel and the right panel display the dependence on t_1 (with t_2 integrated from 0 to $5\tau_D$) and t_2 (with t_1 integrated from 0 to $3\tau_{B_d}$), respectively.

We perform numerical analysis on this channel. As depicted in the left panel of **Figure 9**, the peak of the two-dimensional time-dependent double-mixing results is on the order of 10^{-2} , occurring at later t_2 and earlier t_1 times. When integrating t_2 from 0 to $5\tau_D$, the peak value of the double-mixing effect contributes only 0.8% to the total. The dependencies of A_{CP} and A_{dm} on t_1 are similar, differing only in amplitude magnitude. Upon integrating t_1 from 0 to $3\tau_{B_d}$, the t_2 dependence of A_{CP} is shown in the right panel. The dependence of A_{dm} on t_2 is nearly linear, attributed to its nearly hyperbolic sine dependence on t_2 . However, due to the small value of y_D , the overall variation of A_{dm} with t_2 remains nearly linear. The double-mixing CP violation in the decay channel of this meson is relatively more significant than in the $\pi^+\pi^-$ final state, due to the presence of the r_D factor which suppresses the dominant non-double-mixing CP violation terms. The dominant contribution to the non-double-mixing CP violation arises from the interference between the $B_d^0 \rightarrow \bar{D}^0$ and $B_d^0 \rightarrow D^0$ path, *i.e.*, the third line of $A_{non-dm,1}(t_1, t_2)$. A slightly smaller contribution comes from the interference between the $B_d^0 \rightarrow D^0$ and $B_d^0 \rightarrow \bar{B}_d^0 \rightarrow D^0$ paths, *i.e.*, the first term of $A_{non-dm,2}(t_1, t_2)$ which involves the factor r_B . The two-dimensional time integration of $A_{CP}(t_1, t_2)$ for this channel, presented in Table 5, suggests that the CP asymmetry A_{CP} is relatively insensitive to the decay of the D meson.

3.2 B_s^0 decays

In this subsection, we extend our investigation to the B_s^0 meson, by considering decays with the same final states as the B_d^0 decays. For simplicity, we retain the approximation:

$$q_{B_s}/p_{B_s} = e^{-i\phi_{B_s}}. \quad (3.18)$$

Unlike the B_d^0 meson, the B_s^0 meson exhibits a non-negligible difference in decay widths, as indicated in Table 1. Consequently, the double-mixing CP violation for the B_s^0 meson comprises both a component proportional to $\sin \Delta m_{B_s} t_1$, represented by $A_{n,dm}$, and a component proportional to $\sinh \frac{1}{2} \Delta \Gamma_{B_s} t_1$, represented by $A_{h,dm}$. Although the underlying calculation process is similar to that for the B_d^0 meson, the results for the B_s^0 meson are inherently more complicated, implying more fruitful phenomenology.

3.2.1 $B_s^0 \rightarrow J/\psi K \rightarrow J/\psi f_+$

We first consider the process $B_s^0 \rightarrow J/\psi K \rightarrow J/\psi f_+$, which originates from the $\bar{b} \rightarrow \bar{c}c\bar{d}$ quark-level transition. The first observation of such a mode $B_s^0 \rightarrow J/\psi K_S^0$ was reported by CDF along with the measured branching ratio [48]. In this channel, both the transitions $B_s^0 \rightarrow J/\psi \bar{K}^0$ and $B_s^0 \rightarrow \bar{B}_s^0 \rightarrow J/\psi K^0$ can occur, with final state f_+ selected as $\pi^+\pi^-$ being common to both K^0 and \bar{K}^0 , resulting in four possible paths. This makes these channels fall into the second category of our previously defined classifications.

In the calculation of the CP violation of this channel, direct CP violation in the primary and secondary decays are neglected. The involved phase difference between the decay amplitude $\langle J/\psi K^0 | \bar{B}_s^0 \rangle$ and its charge conjugation $\langle J/\psi \bar{K}^0 | B_s^0 \rangle$ is given by $-e^{i\omega_{B_s}} = -(V_{cb}V_{cd}^*)/(V_{cb}^*V_{cd})$, with its numerical value detailed in Table 1. The negative sign arises from the convention $CP |J/\psi K^0\rangle = -|J/\psi \bar{K}^0\rangle$. The double-mixing CP asymmetry is given by

$$A_{n,dm}(t_1, t_2) = 2 \frac{e^{-(\Gamma_{B_s}t_1 + \Gamma_K t_2)}}{D(t_1, t_2)} \left\{ \sinh \frac{1}{2} \Delta\Gamma_K t_2 \sin \Phi_4 \left(\left| \frac{q_K}{p_K} \right| + \left| \frac{p_K}{q_K} \right| \right) \right. \\ \left. + \sin \Delta m_K t_2 \cos \Phi_4 \left(\left| \frac{q_K}{p_K} \right| - \left| \frac{p_K}{q_K} \right| \right) \right\} \sin \Delta m_{B_s} t_1, \quad (3.19)$$

where $\Phi_4 \equiv \omega_{B_s} - \phi_{B_s} - \phi_K$. It is induced by the interference between $B_s^0 \rightarrow \bar{K}^0 \rightarrow \pi^+\pi^-$ and $B_s^0 \rightarrow \bar{B}_s^0 \rightarrow K^0 \rightarrow \bar{K}^0 \rightarrow \pi^+\pi^-$, as well as between the $B_s^0 \rightarrow \bar{K}^0 \rightarrow K^0 \rightarrow \pi^+\pi^-$ and $B_s^0 \rightarrow \bar{B}_s^0 \rightarrow K^0 \rightarrow \pi^+\pi^-$ pathways. The denominator $D(t_1, t_2)$ is obtained from (2.22) - (2.25), where the substitutions $|p_K/q_K| \leftrightarrow |q_K/p_K|$ and $\phi_K \rightarrow -\phi_K$ need to be performed.

We have conducted numerical analyses of this decay channel, obtaining the CP asymmetry and its time dependence, as illustrated in Figure 10. The left panel shows that the maximum value of the two-dimensional time-dependent CP asymmetry can exceed 50%, a substantial value. Integrating the time t_2 from 0 to $2\tau_K$, the middle panel shows the t_1 dependence of A_{CP} . The rapid oscillation observed is due to the large x_s value of the B_s^0 meson. The total CP asymmetry is dominated by the S_n term, which can be further separated into the double-mixing part $A_{n,dm}$ and the non-double-mixing part, both of which have the sine dependence on t_1 , as defined in (2.4). The double-mixing part has a magnitude approximately twice the total CP asymmetry but with an opposite sign. Integrating t_1 from 0 to τ_{B_s} reveals the t_2 dependence of A_{CP} , as shown in the right panel. In this case, A_{CP} is almost zero because the cancellation between the double-mixing and non-double-mixing terms in S_n , while $A_{n,dm}$ varies approximately as $-\exp(y_K t_2) \sinh y_K t_2$ with respect to t_2 .

3.2.2 $B_s^0 \rightarrow J/\psi K \rightarrow J/\psi(\pi^\pm \ell^\mp \nu_\ell)$

The decay process $B_s^0 \rightarrow J/\psi K \rightarrow J/\psi(\pi^-\ell^+\nu_\ell)$ can occur via the two paths $B_s^0 \rightarrow J/\psi \bar{K}^0 \rightarrow J/\psi K^0 \rightarrow J/\psi(\pi^-\ell^+\nu_\ell)$ and $B_s^0 \rightarrow \bar{B}_s^0 \rightarrow J/\psi K^0 \rightarrow J/\psi(\pi^-\ell^+\nu_\ell)$; while; the process $B_s^0 \rightarrow J/\psi K \rightarrow J/\psi(\pi^+\ell^-\bar{\nu}_\ell)$ can occur via $B_s^0 \rightarrow J/\psi \bar{K}^0 \rightarrow J/\psi(\pi^+\ell^-\bar{\nu}_\ell)$ and $B_s^0 \rightarrow \bar{B}_s^0 \rightarrow J/\psi K^0 \rightarrow J/\psi \bar{K}^0 \rightarrow J/\psi(\pi^+\ell^-\bar{\nu}_\ell)$. Therefore, they both align with the first category in our prior discussion.

In the calculation of the CP asymmetry of these channels, we still neglect the direct CP violation in both the primary and secondary decays. Then, we have $\langle f | K^0 \rangle = \langle \bar{f} | \bar{K}^0 \rangle$ and

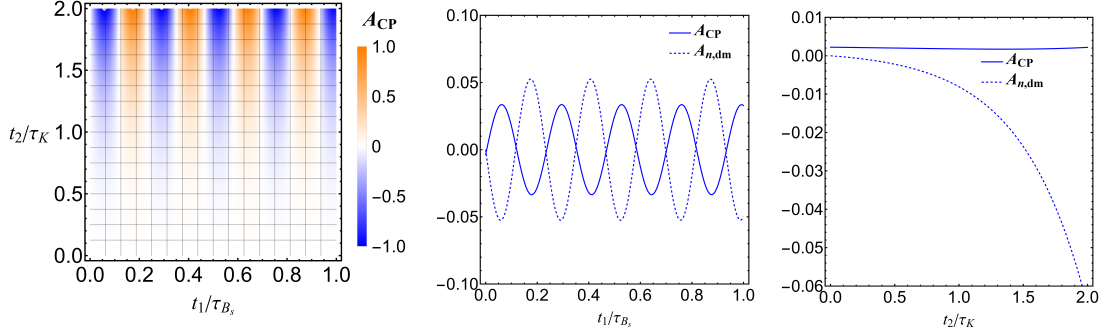


Figure 10. Time dependence of the CP asymmetry A_{CP} in $B_s^0 \rightarrow J/\psi K \rightarrow J/\psi f_+$. The left panel displays the two-dimensional time dependence. The middle panel and the right panel display the dependence on t_1 (with t_2 integrated from 0 to $2\tau_K$) and t_2 (with t_1 integrated from 0 to τ_{B_s}), respectively.

the weak phase difference between the involved primary decay amplitudes is ω_{B_s} as introduced in previously. For the decay channel with the final state $\pi^- \ell^+ \nu_\ell$, the corresponding double-mixing terms are given by

$$A_{h,dm}(t_1, t_2) = -\frac{e^{-(\Gamma_{B_s} t_1 + \Gamma_K t_2)}}{2D(t_1, t_2)} \left\{ \sinh \frac{1}{2} \Delta \Gamma_K t_2 \cos \Phi_4 \left(\left| \frac{p_K}{q_K} \right| - \left| \frac{q_K}{p_K} \right| \right) + \sin \Delta m_K t_2 \sin \Phi_4 \left(\left| \frac{p_K}{q_K} \right| + \left| \frac{q_K}{p_K} \right| \right) \right\} \sinh \frac{1}{2} \Delta \Gamma_{B_s} t_1, \quad (3.20)$$

$$A_{n,dm}(t_1, t_2) = -\frac{e^{-(\Gamma_{B_s} t_1 + \Gamma_K t_2)}}{2D(t_1, t_2)} \left\{ -\sinh \frac{1}{2} \Delta \Gamma_K t_2 \left(\left| \frac{p_K}{q_K} \right| + \left| \frac{q_K}{p_K} \right| \right) \sin \Phi_4 + \sin \Delta m_K t_2 \cos \Phi_4 \left(\left| \frac{p_K}{q_K} \right| - \left| \frac{q_K}{p_K} \right| \right) \right\} \sin \Delta m_{B_s} t_1. \quad (3.21)$$

Combining (2.4) with (2.11) - (2.13) and making the substitutions $|p_K/q_K| \leftrightarrow |q_K/p_K|$ and $\phi_K \rightarrow -\phi_K$ yields the denominator $D(t_1, t_2)$.

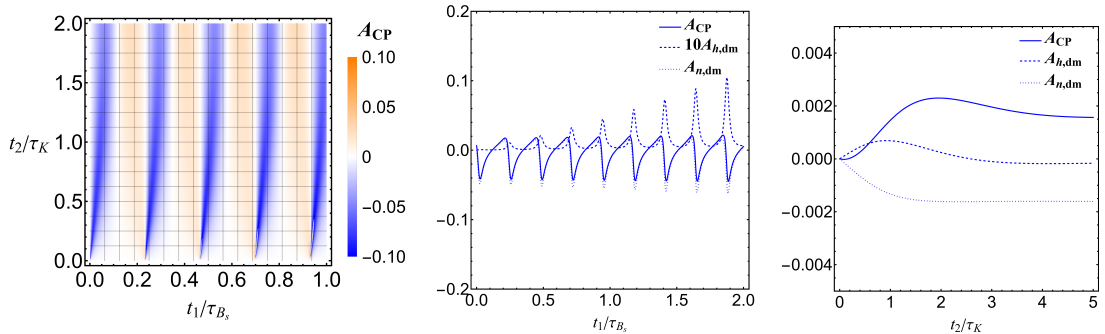


Figure 11. Time dependence of the CP asymmetry A_{CP} in $B_s^0 \rightarrow J/\psi K \rightarrow J/\psi (\pi^- \ell^+ \nu_\ell)$. The left panel displays the two-dimensional time dependence. The middle panel and the right panel display the dependence on t_1 (with t_2 integrated from 0 to τ_K) and t_2 (with t_1 integrated from 0 to $2\tau_{B_s}$), respectively.

The numerical results for the $\pi^-\ell^+\nu_\ell$ channel are illustrated in **Figure 11**. The left panel shows the two-dimensional time dependence of the CP asymmetry, whose maximal values are of $\mathcal{O}(10\%)$. Integrating time t_2 from 0 to τ_K , it is observed from the middle panel that the total asymmetry is dominated by the $A_{n,dm}$ term. This is attributable to the sine dependence on t_1 and hyperbolic sine dependence on t_2 of $A_{n,dm}$, particularly for the large x_s . Conversely, the numerator of $A_{h,dm}$ exhibits a hyperbolic sine dependence on t_1 and a sine dependence on t_2 . In the range of t_1 from 0 to $2\tau_{B_s}$, the numerator of $A_{h,dm}$ increases almost linearly while the denominator behaves like a sine function, so $A_{h,dm}$ experiences modulation over time, as reflected in its increasing peak value. Integrating over t_1 from 0 to $2\tau_{B_s}$, we observe the t_2 dependence of A_{CP} in the right panel of **Figure 11**. Now, the contributions of the C term and $A_{n,dm}$ term are comparable, slightly surpassing the $A_{h,dm}$ term.

When the final state is considered as $\pi^+\ell^-\bar{\nu}_\ell$, the results for the double-mixing terms are similar, but with an extra negative sign in the term $A_{h,dm}$. The corresponding expressions are

$$A_{h,dm}(t_1, t_2) = -\frac{e^{-(\Gamma_{B_s}t_1 + \Gamma_K t_2)}}{2D(t_1, t_2)} \left\{ \sinh \frac{1}{2} \Delta \Gamma_K t_2 \left[\cos \Phi_4 \left(\left| \frac{q_K}{p_K} \right| - \left| \frac{p_K}{q_K} \right| \right) \right] \right. \\ \left. - \sin \Delta m_K t_2 \left[\sin \Phi_4 \left(\left| \frac{q_K}{p_K} \right| + \left| \frac{p_K}{q_K} \right| \right) \right] \right\} \sinh \frac{1}{2} \Delta \Gamma_{B_s} t_1, \quad (3.22)$$

$$A_{n,dm}(t_1, t_2) = -\frac{e^{-(\Gamma_{B_s}t_1 + \Gamma_K t_2)}}{2D(t_1, t_2)} \left\{ -\sinh \frac{1}{2} \Delta \Gamma_K t_2 \left[\sin \Phi_4 \left(\left| \frac{q_K}{p_K} \right| + \left| \frac{p_K}{q_K} \right| \right) \right] \right. \\ \left. - \sin \Delta m_K t_2 \left[\cos \Phi_4 \left(\left| \frac{q_K}{p_K} \right| - \left| \frac{p_K}{q_K} \right| \right) \right] \right\} \sin \Delta m_{B_s} t_1. \quad (3.23)$$

The denominator $D(t_1, t_2)$ can be obtained by combining (2.4) with (2.11) - (2.13), while also performing the substitutions $C'_+(t_2) \leftrightarrow C'_-(t_2)$, $|p_K/q_K| \leftrightarrow |q_K/p_K|$ and $\phi_K \rightarrow -\phi_K$, and adding an extra negative sign in front of $S'_n(t_2)$.

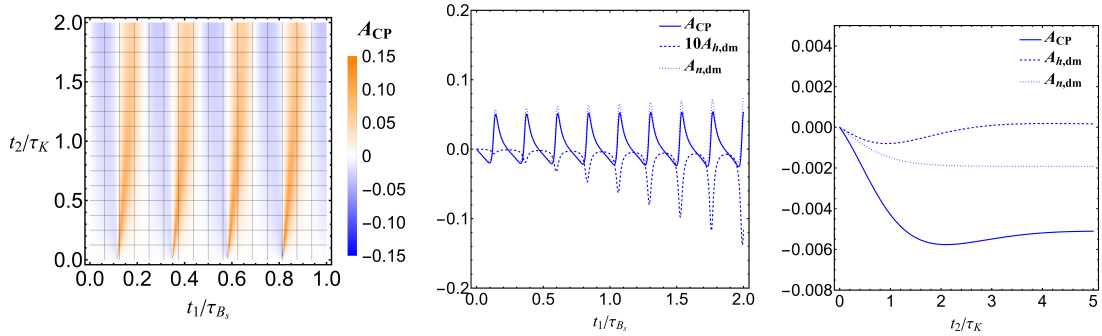


Figure 12. Time dependence of the CP asymmetry A_{CP} in $B_s^0 \rightarrow J/\psi K \rightarrow J/\psi(\pi^+\ell^-\bar{\nu}_\ell)$. The left panel displays the two-dimensional time dependence. The middle panel and the right panel display the dependence on t_1 (with t_2 integrated from 0 to τ_K) and t_2 (with t_1 integrated from 0 to $2\tau_{B_s}$), respectively.

Our numerical analysis for this channel is depicted in **Figure 12**. The left panel presents the two-dimensional time dependence. The difference between the results for this

channel and the $\pi^-\ell^+\nu_\ell$ channel lies in the modulation of the denominator. When t_2 is fixed, the dominant term in the denominator has a hyperbolic cosine dependence on t_1 , which is the same in the results for the two different channels, while the sine term is a secondary contribution, and it contributes to the two channels with a sign difference. The middle panel shows the CP asymmetry with t_2 integrated from 0 to τ_K . While the $A_{n,dm}$ term still dominates, the growth magnitude of the $A_{h,dm}$ term is larger compared to the $\pi^-\ell^+\nu_\ell$ channel. Integrating over t_1 and analyzing t_2 dependence in the right panel, the $A_{h,dm}$ term emerges as dominant. Additionally, both the A_{CP} and $A_{n,dm}$ terms in the $\pi^+\ell^-\bar{\nu}_\ell$ channel display a sign difference from the $\pi^-\ell^+\nu_\ell$ channel.

3.2.3 $B_s^0 \rightarrow \rho^0 K \rightarrow \rho^0(\pi^\pm \ell^\mp \nu)$

The decay processes $B_s^0 \rightarrow \rho^0 K \rightarrow \rho^0(\pi^\pm \ell^\mp \nu)$ resemble to $B_s^0 \rightarrow J/\psi K_{L,S}^0 (\rightarrow \pi^-\ell^+\nu_\ell)$, differing primarily in the phase difference ω_5 . This difference arises from the phase between the decay amplitude $\langle \rho^0 \bar{K}^0 | B_s^0 \rangle$ and its charge conjugate $\langle \rho^0 K^0 | \bar{B}_s^0 \rangle$, contrasting with the phase difference ω_{B_s} in the former. Considering $CP |\rho^0 K^0\rangle = -|\rho^0 \bar{K}^0\rangle$, we define

$$\frac{\langle \rho^0 K^0 | \bar{B}_s^0 \rangle}{\langle \rho^0 \bar{K}^0 | B_s^0 \rangle} = -e^{i\omega_5}, \quad \omega_5 = \arg \frac{V_{ub}V_{ud}^*}{V_{ub}^*V_{ud}}, \quad (3.24)$$

where again we have neglected the direct CP asymmetry in these processes.

For the final state $\pi^-\ell^+\nu_\ell$, two possible paths exist: $B_s^0 \rightarrow \rho^0 \bar{K}^0 \rightarrow \rho^0 K^0 \rightarrow \rho^0(\pi^-\ell^+\nu_\ell)$ and $B_s^0 \rightarrow \bar{B}_s^0 \rightarrow \rho^0 K^0 \rightarrow \rho^0(\pi^-\ell^+\nu_\ell)$. Therefore, it is categorized as the first type in our classification. The results for the double-mixing terms are

$$A_{h,dm}(t_1, t_2) = -\frac{e^{-(\Gamma_{B_s}t_1 + \Gamma_K t_2)}}{2D(t_1, t_2)} \left\{ \left(\left| \frac{p_K}{q_K} \right| - \left| \frac{q_K}{p_K} \right| \right) \cos \Phi_5 \sinh \frac{1}{2} \Delta \Gamma_K t_2 \right. \\ \left. - \left(\left| \frac{p_K}{q_K} \right| + \left| \frac{q_K}{p_K} \right| \right) \sin \Phi_5 \sin \Delta m_K t_2 \right\} \sinh \frac{1}{2} \Delta \Gamma_{B_s} t_1, \quad (3.25)$$

$$A_{n,dm}(t_1, t_2) = -\frac{e^{-(\Gamma_{B_s}t_1 + \Gamma_K t_2)}}{2D(t_1, t_2)} \left\{ \left(\left| \frac{p_K}{q_K} \right| + \left| \frac{q_K}{p_K} \right| \right) \sin \Phi_5 \sinh \frac{1}{2} \Delta \Gamma_K t_2 \right. \\ \left. + \left(\left| \frac{p_K}{q_K} \right| - \left| \frac{q_K}{p_K} \right| \right) \cos \Phi_5 \sin \Delta m_K t_2 \right\} \sin \Delta m_{B_s} t_1, \quad (3.26)$$

where $\Phi_5 \equiv \phi_{B_s} + \phi_K - \omega_5$. $D(t_1, t_2)$ can be obtained by replacing ω_{B_s} in the denominator of (3.20) with ω_5 .

We have conducted the numerical analysis of both the total CP asymmetry A_{CP} and the double-mixing CP asymmetry A_{dm} , which are depicted in **Figure 13**. The two-dimensional time-dependent CP violation is depicted in the left panel, showing a peak value exceeding 50%. By integrating t_2 from 0 to τ_K , we obtain the t_1 -dependent results displayed in the middle panel, where the double-mixing CP violation is notably significant. Here, A_{CP} predominantly arises from the double-mixing CP violation, particularly from the $A_{n,dm}$ term, which sums the contributions of the decays of K_S^0 and K_L^0 . Integrating t_1 from τ_{B_s} to $5\tau_{B_s}$ yields the t_2 -dependent results, showcased in the right panel. In this scenario, A_{CP} still mainly originates from the double-mixing CP violation, with the term $A_{h,dm}$ being dominant, particularly governed by the $K_S^0 - K_L^0$ interference.

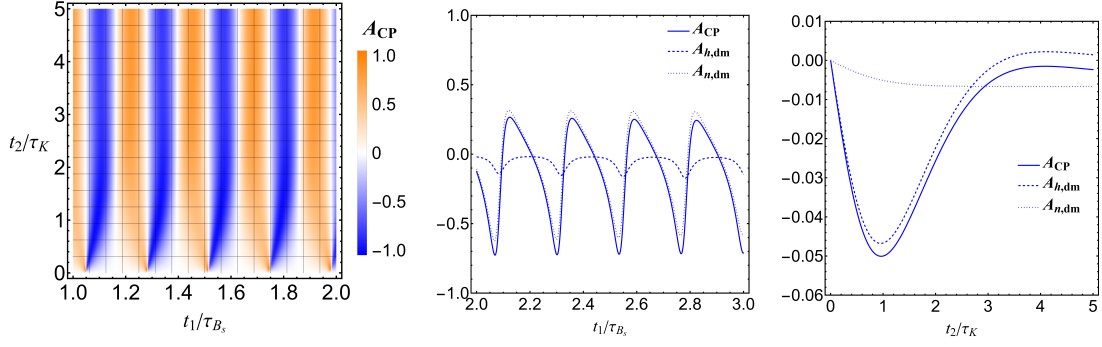


Figure 13. Time dependence of the CP asymmetry A_{CP} in $B_s^0 \rightarrow \rho^0 K \rightarrow \rho^0(\pi^- \ell^+ \nu_\ell)$. The left panel displays the two-dimensional time dependence. The middle panel and the right panel display the dependence on t_1 (with t_2 integrated from 0 to τ_K) and t_2 (with t_1 integrated from τ_{B_s} to $5\tau_{B_s}$), respectively.

The results for the double-mixing terms of the $\pi^+ \ell^- \bar{\nu}_\ell$ channel are similar to those of the $\pi^- \ell^+ \nu_\ell$ channel with an extra overall negative sign in the term $A_{h,dm}$. They are calculated as

$$A_{h,dm}(t_1, t_2) = - \frac{e^{-(\Gamma_{B_s} t_1 + \Gamma_K t_2)}}{2D(t_1, t_2)} \left\{ \sinh \frac{1}{2} \Delta \Gamma_K t_2 \left[\cos \Phi_5 \left(\left| \frac{q_K}{p_K} \right| - \left| \frac{p_K}{q_K} \right| \right) \right] + \sin \Delta m_K t_2 \left[\sin \Phi_5 \left(\left| \frac{q_K}{p_K} \right| + \left| \frac{p_K}{q_K} \right| \right) \right] \right\} \sinh \frac{1}{2} \Delta \Gamma_{B_s} t_1, \quad (3.27)$$

$$A_{n,dm}(t_1, t_2) = - \frac{e^{-(\Gamma_{B_s} t_1 + \Gamma_K t_2)}}{2D(t_1, t_2)} \left\{ \sinh \frac{1}{2} \Delta \Gamma_K t_2 \left[\sin \Phi_5 \left(\left| \frac{q_K}{p_K} \right| + \left| \frac{p_K}{q_K} \right| \right) \right] - \sin \Delta m_K t_2 \left[\cos \Phi_5 \left(\left| \frac{q_K}{p_K} \right| - \left| \frac{p_K}{q_K} \right| \right) \right] \right\} \sin \Delta m_{B_s} t_1, \quad (3.28)$$

where the denominator $D(t_1, t_2)$ can be obtained from the denominator of (3.22) by replacing ω_{B_s} with ω_5 .

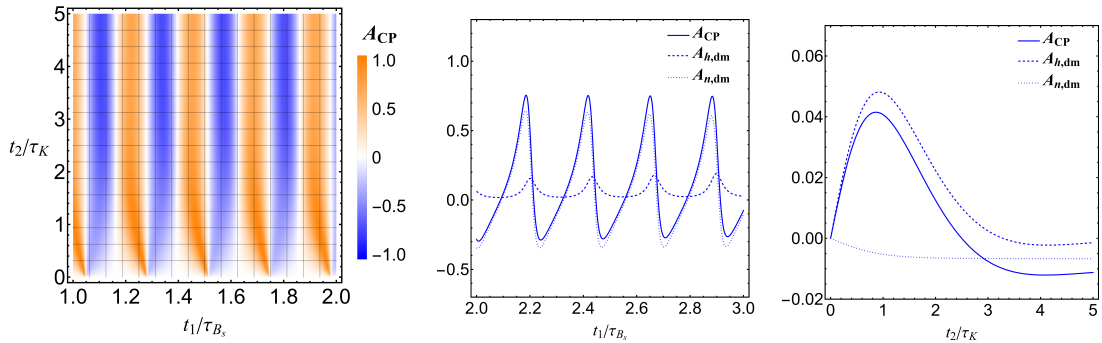


Figure 14. Time dependence of the CP asymmetry A_{CP} in $B_s^0 \rightarrow \rho^0 K \rightarrow \rho^0(\pi^+ \ell^- \bar{\nu}_\ell)$. The left panel displays the two-dimensional time dependence. The middle panel and the right panel display the dependence on t_1 (with t_2 integrated from 0 to τ_K) and t_2 (with t_1 integrated from τ_{B_s} to $5\tau_{B_s}$), respectively.

Our analysis for this channel reveals a smaller CP violation compared to the $\pi^-\ell^+\nu_\ell$ final state, as displayed in **Figure 14**. The left panel displays the two-dimensional time dependence of the CP asymmetry. Integrating t_2 from 0 to τ_K , the t_1 -dependent results, depicted in the middle panel, highlight the dominant role of separate contributions from K_S^0 and K_L^0 in the double-mixing CP violation. When integrating t_1 from τ_{B_s} to $5\tau_{B_s}$, the t_2 -dependent results, as shown in the right panel, are predominantly influenced by the $K_S^0 - K_L^0$ interference. Notably, the value of the t_1 -integrated CP violation is almost entirely positive, contrasting with the result for the $\pi^-\ell^+\nu_\ell$ final state. This distinction enables the experimental differentiation of these two processes.

We emphasize that the best approach for the first experimental attempt to measure the double-mixing CP violation would be to combine the two decay channels mentioned above. Considering the CP violation defined by the differences of the summed branching ratios

$$\frac{\mathcal{B}[B_s^0/\bar{B}_s^0 \rightarrow \rho^0 K \rightarrow \rho^0(\pi^-\ell^+\nu_\ell)] - \mathcal{B}[B_s^0/\bar{B}_s^0 \rightarrow \rho^0 K \rightarrow \rho^0(\pi^+\ell^-\bar{\nu}_\ell)]}{\mathcal{B}[B_s^0/\bar{B}_s^0 \rightarrow \rho^0 K \rightarrow \rho^0(\pi^-\ell^+\nu_\ell)] + \mathcal{B}[B_s^0/\bar{B}_s^0 \rightarrow \rho^0 K \rightarrow \rho^0(\pi^+\ell^-\bar{\nu}_\ell)]}, \quad (3.29)$$

initial tagging for B mesons in experiments is not necessary and the corresponding efficiency loss is prevented. It contains the double-mixing and non-double-mixing terms, which are calculated to be

$$A_{h,dm}(t_1, t_2) = -\frac{e^{-(\Gamma_{B_s}t_1 + \Gamma_K t_2)}}{D(t_1, t_2)} \left\{ \sinh \frac{1}{2} \Delta \Gamma_K t_2 \cos \Phi_5 \left(\left| \frac{p_K}{q_K} \right| - \left| \frac{q_K}{p_K} \right| \right) - \sin \Delta m_K t_2 \sin \Phi_5 \left(\left| \frac{p_K}{q_K} \right| + \left| \frac{q_K}{p_K} \right| \right) \right\} \sinh \frac{1}{2} \Delta \Gamma_{B_s} t_1, \quad (3.30)$$

$$A_{non-dm}(t_1, t_2) = \frac{e^{-\Gamma_{B_s} t_1}}{D(t_1, t_2)} \left(\left| \frac{p_K}{q_K} \right|^2 - \left| \frac{q_K}{p_K} \right|^2 \right) |g_{-,K}(t_2)|^2 \cosh \frac{1}{2} \Delta \Gamma_{B_s} t_1, \quad (3.31)$$

$$D(t_1, t_2) = e^{-\Gamma_{B_s} t_1} \left\{ \left(\left| \frac{p_K}{q_K} \right|^2 + \left| \frac{q_K}{p_K} \right|^2 \right) |g_{-,K}(t_2)|^2 + 2|g_{+,K}(t_2)|^2 \right\} \cosh \frac{1}{2} \Delta \Gamma_{B_s} t_1 - e^{-(\Gamma_{B_s} t_1 + \Gamma_K t_2)} \left\{ \sinh \frac{1}{2} \Delta \Gamma_K t_2 \cos \Phi_5 \left(\left| \frac{p_K}{q_K} \right| + \left| \frac{q_K}{p_K} \right| \right) - \sin \Delta m_K t_2 \sin \Phi_5 \left(\left| \frac{p_K}{q_K} \right| - \left| \frac{q_K}{p_K} \right| \right) \right\} \sinh \frac{1}{2} \Delta \Gamma_{B_s} t_1. \quad (3.32)$$

Apparently, the non-double-mixing term is negligible and the total CP violation is dominated by the double-mixing contribution.

We conducted a numerical analysis of this process, and the results are depicted in **Figure 15**. The left panel exhibits that the total CP asymmetry has a hyperbolic tangent dependence on t_1 , consequently behaving linearly when t_1 is not too large. When integrating t_2 from 0 to τ_K , the total CP violation is predominantly contributed from the double-mixing CP violation, as displayed in the middle panel. It exhibits a linear dependence on t_1 , which is consistent with the two-dimensional time dependence. The right panel shows the variation of CP violation with respect to t_2 after integrating t_1 from τ_{B_s} to $5\tau_{B_s}$. As t_2 increases, it first reaches a maximum and then rapidly decreases to nearly zero. This is because the primary contribution of the double-mixing CP violation in the numerator comes from the interference term between K_S^0 and K_L^0 , *i.e.*, the second term in (3.32), which has a sine

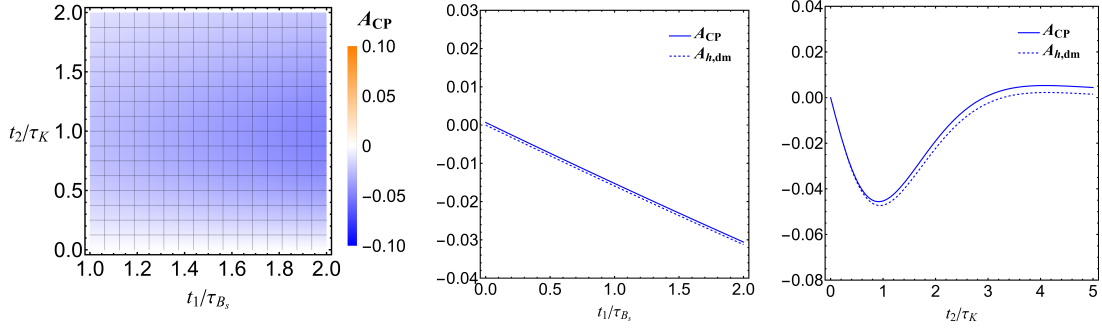


Figure 15. Time dependence of the CP asymmetry A_{CP} in $B_s^0(t_1) \rightarrow \rho^0 K(t_2) \rightarrow \rho^0(\pi\ell\nu)$ defined by (3.29). The left panel displays the two-dimensional time dependence. The middle panel and the right panel display the dependence on t_1 (with t_2 integrated from 0 to τ_K) and t_2 (with t_1 integrated from τ_{B_s} to $5\tau_{B_s}$), respectively.

t_1/τ_{B_s}	t_2/τ_K	A_{CP}
0~3	0~ 2	-1.33%
0~2	0~ 2	-1.06%
0~3	0~ 1	-1.28%
0~2	0~ 1	-1.03%
0~3	0~ 0.5	-0.83%
0~2	0~ 0.5	-0.67%

Table 6. The time integrated A_{CP} in $B_s^0 \rightarrow \rho^0 K \rightarrow \rho^0(\pi\ell\nu_\ell)$.

dependence on t_2 . Meanwhile, the denominator is mainly contributed by the term that depends on the hyperbolic cosine function of t_2 , which continues to increase with time. The time-integrated results for the CP asymmetry (3.29) for this case are presented in Table 6, for experimental convenience. With different integrated time ranges, the values are basically around -1%.

3.2.4 $B_s^0 \rightarrow DK \rightarrow (K^-\pi^+)(\pi^-\ell^+\nu_\ell)$

We now focus on the decay channel $B_s^0 \rightarrow DK \rightarrow (K^-\pi^+)(\pi^-\ell^+\nu_\ell)$. This process involves four paths, even when we neglect the small mixing of the neutral D meson: $B_s^0 \rightarrow D^0\bar{K}^0 \rightarrow D^0K^0 \rightarrow f$, $B_s^0 \rightarrow \bar{D}^0\bar{K}^0 \rightarrow \bar{D}^0K^0 \rightarrow f$, $B_s^0 \rightarrow \bar{B}_s^0 \rightarrow D^0K^0 \rightarrow f$ and $B_s^0 \rightarrow \bar{B}_s^0 \rightarrow \bar{D}^0K^0 \rightarrow f$, where $f \equiv (K^-\pi^+)(\pi\ell\nu)$. This situation is very unique and does not belong to any of the categories we previously defined, but the expression for the CP violation can be derived analogously. We define the ratios between the decay amplitudes as

$$\begin{aligned}
\frac{A(\bar{B}_s^0 \rightarrow D^0K^0)}{A(B_s^0 \rightarrow \bar{D}^0\bar{K}^0)} &= e^{i\omega_3}, \quad \omega_3 = \arg \frac{V_{cb}V_{ud}^*}{V_{cb}^*V_{ud}}, \\
\frac{A(B_s^0 \rightarrow D^0\bar{K}^0)}{A(B_s^0 \rightarrow \bar{D}^0\bar{K}^0)} &= r e^{i(\delta_4+\omega_4)}, \quad \omega_4 = \arg \frac{V_{ub}^*V_{cd}}{V_{cb}^*V_{ud}},
\end{aligned} \tag{3.33}$$

where $\omega_{3,4}$ are the weak phases and δ_4 is the strong phase. Then, the double-mixing and non-double-mixing CP violation terms defined in (2.4) are calculated as

$$\begin{aligned}
A_{h,dm}(t_1, t_2) &= \frac{N_1}{D(t_1, t_2)} \\
&= \frac{e^{-(\Gamma_{B_s} t_1 + \Gamma_K t_2)}}{2D(t_1, t_2)} \left| \frac{p_K}{q_K} \right| \left\{ \sinh \frac{\Delta \Gamma_K t_2}{2} [r \cos(\delta_4 + \Phi_6) - r_D \cos(\Phi_7 - \delta_D)] \right. \\
&\quad \left. + \sin \Delta m_K t_2 [-r \sin(\delta_4 + \Phi_6) + r_D \sin(\Phi_7 - \delta_D)] \right\} \sinh \frac{\Delta \Gamma_{B_s} t_1}{2} \\
&\quad - \frac{e^{-(\Gamma_{B_s} t_1 + \Gamma_K t_2)}}{2D(t_1, t_2)} \left| \frac{q_K}{p_K} \right| \left\{ \sinh \frac{\Delta \Gamma_K t_2}{2} [r \cos(\delta_4 - \Phi_6) - r_D \cos(\Phi_7 + \delta_D)] \right. \\
&\quad \left. + \sin \Delta m_K t_2 [-r \sin(\delta_4 - \Phi_6) - r_D \sin(\Phi_7 + \delta_D)] \right\} \sinh \frac{\Delta \Gamma_{B_s} t_1}{2} \\
&\quad - \frac{e^{-(\Gamma_{B_s} t_1 + \Gamma_K t_2)}}{2D(t_1, t_2)} \left| \frac{p_K}{q_K} \right| r r_D \left\{ \sinh \frac{\Delta \Gamma_K t_2}{2} (r \cos(\Phi_8 - \delta_D) - r_D \cos(\delta_4 - \Phi_6)) \right. \\
&\quad \left. + \sin \Delta m_K t_2 (r \sin(\Phi_8 - \delta_D) - r_D \sin(\delta_4 - \Phi_6)) \right\} \sinh \frac{\Delta \Gamma_{B_s} t_1}{2} \\
&\quad + \frac{e^{-(\Gamma_{B_s} t_1 + \Gamma_K t_2)}}{2D(t_1, t_2)} r r_D \left| \frac{q_K}{p_K} \right| \sinh \frac{\Delta \Gamma_{B_s} t_1}{2} \times \\
&\quad \left\{ r \left(\sinh \frac{\Delta \Gamma_K t_2}{2} \cos(\Phi_8 + \delta_D) - \sin \Delta m_K t_2 \sin(\Phi_8 + \delta_D) \right) \right. \\
&\quad \left. - r_D \left(\sinh \frac{\Delta \Gamma_K t_2}{2} \cos(\delta_4 + \Phi_6) + \sin \Delta m_K t_2 \sin(\delta_4 + \Phi_6) \right) \right\}, \tag{3.34}
\end{aligned}$$

$$\begin{aligned}
A_{n,dm}(t_1, t_2) &= \frac{N_2}{D(t_1, t_2)} \\
&= \frac{e^{-(\Gamma_{B_s} t_1 + \Gamma_K t_2)}}{2D(t_1, t_2)} \left| \frac{p_K}{q_K} \right| \left\{ \sinh \frac{\Delta \Gamma_K t_2}{2} [r \sin(\delta_4 + \Phi_6) - r_D \sin(\Phi_7 - \delta_D)] \right. \\
&\quad \left. + \sin \Delta m_K t_2 [r \cos(\delta_4 + \Phi_6) - r_D \cos(\Phi_7 - \delta_D)] \right\} \sin \Delta m_{B_s} t_1 \\
&\quad - \frac{e^{-(\Gamma_{B_s} t_1 + \Gamma_K t_2)}}{2D(t_1, t_2)} \left| \frac{q_K}{p_K} \right| \left\{ \sinh \frac{\Delta \Gamma_K t_2}{2} [r \sin(\delta_4 - \Phi_6) + r_D \sin(\Phi_7 + \delta_D)] \right. \\
&\quad \left. + \sin \Delta m_K t_2 [r \cos(\delta_4 - \Phi_6) - r_D \cos(\Phi_7 + \delta_D)] \right\} \sin \Delta m_{B_s} t_1 \\
&\quad - \frac{e^{-(\Gamma_{B_s} t_1 + \Gamma_K t_2)}}{2D(t_1, t_2)} \left| \frac{p_K}{q_K} \right| r r_D \left\{ \sinh \frac{\Delta \Gamma_K t_2}{2} [-r \sin(\Phi_8 - \delta_D) + r_D \sin(\delta_4 - \Phi_6)] \right. \\
&\quad \left. + \sin \Delta m_K t_2 [r \cos(\Phi_8 - \delta_D) - r_D \cos(\delta_4 - \Phi_6)] \right\} \sin \Delta m_{B_s} t_1 \\
&\quad + \frac{e^{-(\Gamma_{B_s} t_1 + \Gamma_K t_2)}}{2D(t_1, t_2)} r r_D \left| \frac{q_K}{p_K} \right| \sin \Delta m_{B_s} t_1 \times \\
&\quad \left\{ r \left(\sinh \frac{\Delta \Gamma_K t_2}{2} \sin(\Phi_8 + \delta_D) + \sin \Delta m_K t_2 \cos(\Phi_8 + \delta_D) \right) \right. \\
&\quad \left. + r_D \left(\sinh \frac{\Delta \Gamma_K t_2}{2} \sin(\delta_4 + \Phi_6) - \sin \Delta m_K t_2 \cos(\delta_4 + \Phi_6) \right) \right\}, \tag{3.35}
\end{aligned}$$

$$\begin{aligned}
A_{non-dm}(t_1, t_2) &= \frac{N_3}{D(t_1, t_2)} \\
&= \left\{ |g_{+,B_s}(t_1)|^2 |g_{-,K}(t_2)|^2 \left\{ \left| \frac{p_K}{q_K} \right|^2 [r^2 + r_D^2 - 2r_D r \cos(\delta_4 + \delta_D + \omega_4)] \right. \right. \\
&\quad \left. \left. - \left| \frac{q_K}{p_K} \right|^2 [r^2 + r_D^2 - 2r_D r \cos(\delta_4 + \delta_D - \omega_4)] \right\} - 2r_D r |g_{+,K}(t_2)|^2 \times \right. \\
&\quad \left. [\cos(\delta_4 - \omega_4 - \delta_D) - \cos(\delta_4 + \omega_4 - \delta_D)] |g_{-,B_s}(t_1)|^2 \right\} \frac{1}{D(t_1, t_2)}, \quad (3.36)
\end{aligned}$$

where $\Phi_6 \equiv \phi_{B_s} + \phi_K - \omega_3 + \omega_4$, $\Phi_7 \equiv \phi_{B_s} + \phi_K - \omega_3$ and $\Phi_8 \equiv -\phi_{B_s} - \phi_K + \omega_3 - 2\omega_4$. The denominator $D(t_1, t_2)$ can be divided into three parts $N'_1 + N'_2 + N'_3$, which can be obtained by make some replacements to N_1 , N_2 , and N_3 in (3.34) - (3.36). N'_1 and N'_2 can be obtained by changing the sign in front of the exponential in the fourth line and the third-to-last line of (3.34) and (3.35) to an opposite sign. As for N'_3 , in addition to changing the minus sign in front of $|q_K/p_K|^2$ in the third line and the minus sign between the two cosines in the fourth line of (3.36) to a positive sign in N_3 , we still need to incorporate an additional term $2|g_{-,B_s}(t_1)|^2 |g_{+,K}(t_2)|^2 (r_D^2 r^2 + 1)$ to the modified N_3 .

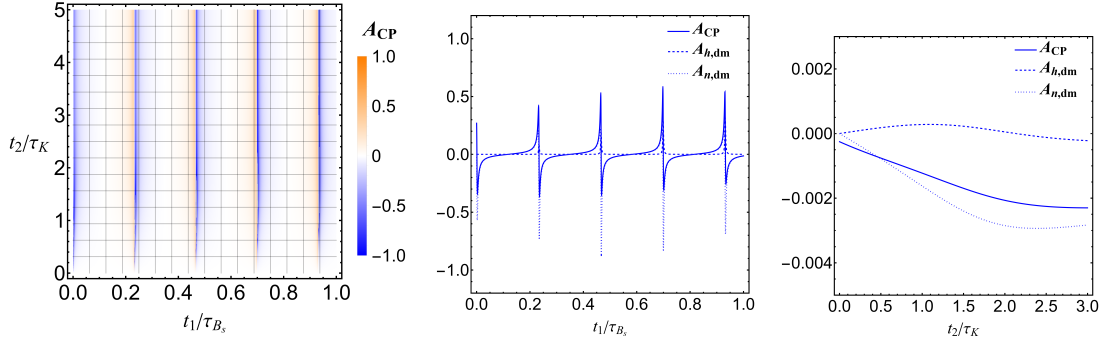


Figure 16. Time dependence of the CP asymmetry A_{CP} in $B_s^0 \rightarrow DK \rightarrow (K^- \pi^+) (\pi^- \ell^+ \nu_\ell)$. The left panel displays the two-dimensional time dependence. The middle panel and the right panel display the dependence on t_1 (with t_2 integrated from 0 to $2\tau_K$) and t_2 (with t_1 integrated from 0 to τ_{B_s}), respectively.

The numerical result of the CP asymmetry in this process is shown in **Figure 16**. The two-dimensional time-dependent CP violation is shown in the left panel. While its peaks surpass 50%, it is only present in the proximity of specific moments. The result of integrating t_2 from 0 to $2\tau_K$ is shown in the middle panel. The contribution of $A_{n,dm}$ dominates except at the positions of positive peaks, as the values of $A_{h,dm}$ and A_{non-dm} are both positive and form upward pulses at each peak position, while $A_{n,dm}$ rapidly rises at each peak position and then directly becomes a negative pulse. Additionally, as the sum of $A_{h,dm}$ and A_{non-dm} is positive when $A_{n,dm}$ is negative, and their contribution is smaller than $A_{n,dm}$, the overall CP violation A_{CP} has larger positive peaks and smaller negative peaks compared to $A_{n,dm}$. The result of integrating t_1 from 0 to τ_{B_s} is shown in the right panel. $A_{h,dm}$ is one order of magnitude smaller than $A_{n,dm}$. The interference between $B_s^0 \rightarrow D^0 \bar{K}^0 \rightarrow D^0 K^0$ and $B_s^0 \rightarrow \bar{B}_s^0 \rightarrow D^0 K^0$ is suppressed by the factor r .

Considering the contribution from \bar{D}^0 , the interference between $B_s^0 \rightarrow \bar{D}^0 \bar{K}^0 \rightarrow \bar{D}^0 K^0$ and $B_s^0 \rightarrow \bar{B}_s^0 \rightarrow D^0 K^0$ is suppressed by r_D , while the remaining interference contributions are all suppressed by factors of rr_D or even more suppressed.

3.2.5 $B_s^0 \rightarrow DK_S^0 \rightarrow (\pi^+\pi^-)K_S^0$ and $B_s^0 \rightarrow DK_S^0 \rightarrow (K^-\pi^+)K_S^0$

We now analyze the decay modes $B_s^0 \rightarrow DK_S^0 \rightarrow f_D K_S^0$, with $f_D = \pi^+\pi^-, K^-\pi^+$. Measurements of similar channels have been performed by experiments. The branching ratio of $B_s^0 \rightarrow \bar{D}^0 \bar{K}^{*0}$ has been reported by LHCb [49, 50], but the final state is self-tagged by the flavor of the K^{*0} , which excludes time-dependent analysis. The CP violation for $A_{CP}(B_s^0 \rightarrow f_D K^{*0})$ has been measured [51]. Considering the possible decays $B_s^0 \rightarrow D^0 K_S^0$, $B_s^0 \rightarrow \bar{D}^0 K_S^0$, $D^0 \rightarrow f_D$, and $\bar{D}^0 \rightarrow f_D$, there are eight pathways for these two process, fitting them into what is defined as the third type.

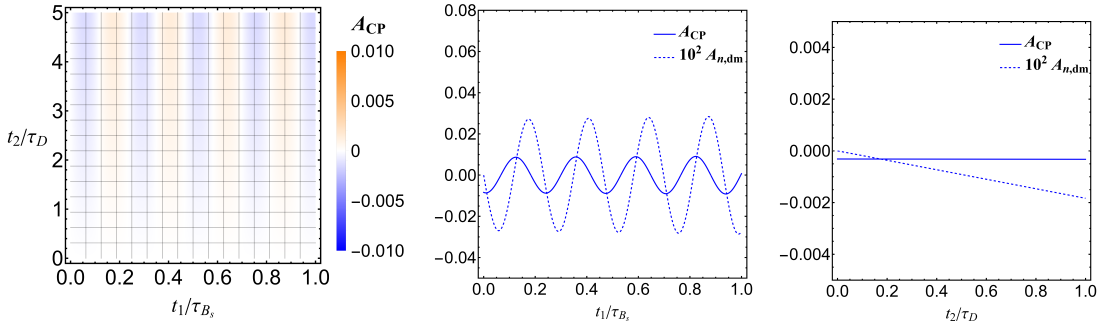


Figure 17. Time dependence of the CP asymmetry A_{CP} in $B_s^0 \rightarrow DK_S^0 \rightarrow (\pi^+\pi^-)K_S^0$. The left panel displays the two-dimensional time dependence. The middle panel and the right panel display the dependence on t_1 (with t_2 integrated from 0 to $5\tau_D$) and t_2 (with t_1 integrated from 0 to τ_{B_s}), respectively.

For the channel with $f_D = \pi^+\pi^-$, we derive the results for all the components of CP violation by setting $r_1 = r$, $\delta_1 = \delta_4$, $\theta_1 = \omega_4$, $\theta_2 = 0$, $r_2 = 1$, $\delta_2 = 0$ and $\theta_3 = \omega_3$ in (2.26), and then we obtain all the terms, which are shown in (A.1) - (A.12). For r and δ_4 defined in (3.33), we numerically use $r = 0.02$ and $\delta_4 = 194^\circ$ as a benchmark. The values for ω_3 and ω_4 are given in Table 1. In this case, the dominant term in the double-mixing CP violation arises from the interference between the $B_s^0 \rightarrow \bar{D}^0 K_S^0 \rightarrow (\pi^+\pi^-)K_S^0$ and $B_s^0 \rightarrow \bar{B}_s^0 \rightarrow D^0 K_S^0 \rightarrow \bar{D}^0 K_S^0 \rightarrow (\pi^+\pi^-)K_S^0$ amplitudes as well as that between the $B_s^0 \rightarrow \bar{D}^0 K_S^0 \rightarrow D^0 K_S^0 \rightarrow (\pi^+\pi^-)K_S^0$ and $B_s^0 \rightarrow \bar{B}_s^0 \rightarrow D^0 K_S^0 \rightarrow (\pi^+\pi^-)K_S^0$ amplitudes. Our numerical results for this channel are presented in Figure 17, with the two-dimensional time dependence in the left panel. Its peak value is $\mathcal{O}(10^{-3})$. Integrating t_2 from 0 to $5\tau_D$ yields the t_1 -dependent result, shown in the middle panel, revealing the double-mixing CP violation effect is of the order $\mathcal{O}(10^{-4})$. This is due to the small values x_D and y_D of the D meson as listed in Table 1. The t_2 -integrated CP asymmetry is dominated by terms arising from the interference between the $B_s^0 \rightarrow \bar{D}^0 K_S^0 \rightarrow (\pi^+\pi^-)K_S^0$ and $B_s^0 \rightarrow \bar{B}_s^0 \rightarrow D^0 K_S^0 \rightarrow (\pi^+\pi^-)K_S^0$ amplitudes, which have a cosine or hyperbolic cosine dependence on t_2 and have a sine dependence on t_1 , namely $\sin \Delta m_{B_s} t_1$. Integrating t_1 from 0 to τ_{B_s} , the magnitude of the double-mixing term $A_{n,dm}$ climbs slowly as t_2 increases attributed to small mixing

parameters of D meson, and the total asymmetry A_{CP} does not show visible changes before t_2 becomes too large, as depicted in the right panel.

For the channel with $f_D = K^-\pi^+$, the double-mixing and non-double-mixing contributions to the CP asymmetry can be obtained by taking (3.16) and (3.17) with the substitutions $\phi_{B_d} \rightarrow \phi_{B_s}$, $r_B \rightarrow r$ and $\delta_B \rightarrow \delta_4$, and the replacement of the denominator $D(t_1, t_2)$ accordingly. For r and δ_4 , we still numerically use $r = 0.02$ and $\delta_4 = 194^\circ$. The presence of the suppression factor r_D and the strong phase δ_D results in a pattern distinct from that of the $\pi^+\pi^-$ channel. The numerical analysis for the double-mixing CP asymmetry A_{dm} is depicted in **Figure 18**. The left panel shows the two-dimensional time dependence, indicating the insignificance of the CP violation with $t_2 < 3\tau_D$, below the threshold of current experimental detection capacities. This double-mixing effect is also negligible in the integrated results over t_2 or t_1 , presented on the middle and the right panel, respectively.

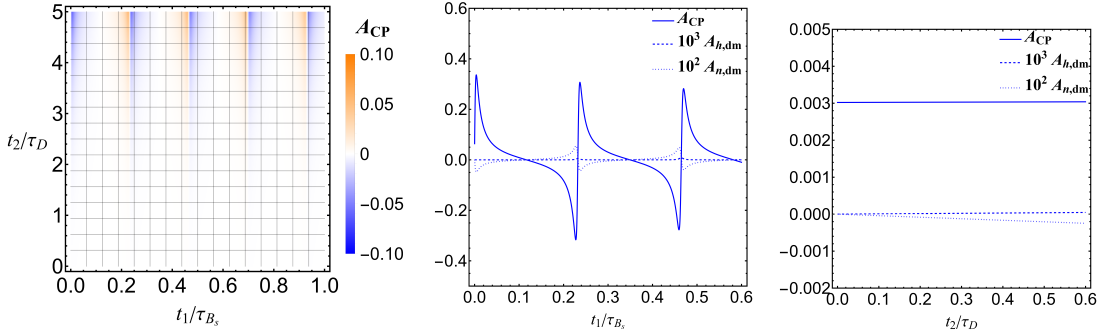


Figure 18. Time dependence of the CP asymmetry A_{CP} in $B_s^0 \rightarrow DK_S^0 \rightarrow (K^-\pi^+)K_S^0$. The left panel displays the two-dimensional time dependence. The middle panel and the right panel display the dependence on t_1 (with t_2 integrated from 0 to $5\tau_D$) and t_2 (with t_1 integrated from 0 to τ_{B_s}), respectively.

4 Conclusions

It was proposed recently by [37] that a long-overlooked CP violation effect exists in a decay chain with two neutral mesons involved, namely the double-mixing CP violation. This violation is induced by the interference among different oscillation paths of two neutral flavored mesons. In this work, we have analyzed the double-mixing CP violation in a series of cascade decay processes $M_1^0(t_1) \rightarrow M_2(t_2) \rightarrow f$, where the primary neutral meson M_1^0 is either $B_{d,s}^0$ mesons and the secondary neutral meson is D^0 or K^0 mesons. The involvement of two time parameters, t_1 and t_2 , makes the two-dimensional time analysis of double-mixing CP violation allowable. We performed numerical analyses for each decay channel, providing the two-dimensional time-dependent double-mixing CP violation and the CP violation integrated over t_1 or t_2 .

Our results show that the double-mixing CP violation can be very significant, with instances exceeding 50% – notably in the decay channel $B_s^0 \rightarrow \rho^0 K \rightarrow \rho^0(\pi\ell\nu)$. In similar cases with kaons reconstructed by semi-leptonic states, the total CP violation almost

entirely comes from the double-mixing CP violation. Moreover, our findings indicate that the double-mixing CP violation's dependency varies distinctly with t_1 and t_2 : when integrating over t_2 , the direct decays of K_S^0 and K_L^0 predominantly contribute to the CP violation, whereas integrating over t_1 highlights the dominance of $K_S^0 - K_L^0$ interference. We emphasize that one of the first experimental attempts to measure the double-mixing CP violation would be to combine the two decay channels $B_s^0 \rightarrow \rho^0 K \rightarrow \rho^0(\pi^-\ell^+\nu_\ell)$ and $B_s^0 \rightarrow \rho^0 K \rightarrow \rho^0(\pi^+\ell^-\bar{\nu}_\ell)$. This method does not require initial tagging of neutral B mesons, thus avoiding efficiency losses.

In comparison, the significance of double-mixing CP violation is less in decay channels involving D^0 as M_2^0 , mainly due to the tiny mixing observed in neutral D mesons, such as in the decay channel $B_s^0 \rightarrow DK_S^0 \rightarrow (\pi^+\pi^-)K_S^0$. Nonetheless, double-mixing CP violation offers a major advantage by facilitating the extraction of CKM phase angles without theoretical inputs. For example, the decay channel $B_d^0 \rightarrow DK \rightarrow (K^-\pi^+)(\pi\ell\nu)$ involves both strong and weak phases, with the overall weak phase being approximated by $2\beta + \gamma$. This allows for the simultaneous extraction of strong and weak phases from experimental data on double-mixing CP violation, thereby directly testing the CKM mechanism.

Acknowledgement

The authors are grateful to Cai-Dian Lü, Wen-Bin Qian, Liang Sun, and Yue-Hong Xie for useful discussions. This work is supported by the Natural Science Foundation of China under grant No. 12375086.

References

- [1] A. D. Sakharov, Pisma Zh. Eksp. Teor. Fiz. **5** (1967), 32-35
- [2] W. Bernreuther, Lect. Notes Phys. **591** (2002), 237-293 [arXiv:hep-ph/0205279 [hep-ph]].
- [3] L. Canetti, M. Drewes and M. Shaposhnikov, New J. Phys. **14** (2012), 095012 [arXiv:1204.4186 [hep-ph]].
- [4] N. Cabibbo, Phys. Rev. Lett. **10** (1963), 531-533
- [5] M. Kobayashi and T. Maskawa, Prog. Theor. Phys. **49** (1973), 652-657
- [6] J. H. Christenson, J. W. Cronin, V. L. Fitch and R. Turlay, Phys. Rev. Lett. **13** (1964), 138-140
- [7] H. Burkhardt *et al.* [NA31], Phys. Lett. B **206** (1988), 169-176
- [8] V. Fanti *et al.* [NA48], Phys. Lett. B **465** (1999), 335-348 [arXiv:hep-ex/9909022 [hep-ex]].
- [9] A. Alavi-Harati *et al.* [KTeV], Phys. Rev. Lett. **83** (1999), 22-27 [arXiv:hep-ex/9905060 [hep-ex]].
- [10] B. Aubert *et al.* [BaBar], Phys. Rev. Lett. **87** (2001), 091801 [arXiv:hep-ex/0107013 [hep-ex]].
- [11] K. Abe *et al.* [Belle], Phys. Rev. Lett. **87** (2001), 091802 [arXiv:hep-ex/0107061 [hep-ex]].
- [12] Y. Chao *et al.* [Belle], Phys. Rev. Lett. **93** (2004), 191802 [arXiv:hep-ex/0408100 [hep-ex]].
- [13] B. Aubert *et al.* [BaBar], Phys. Rev. Lett. **93** (2004), 131801 [arXiv:hep-ex/0407057 [hep-ex]].

- [14] P. del Amo Sanchez *et al.* [BaBar], Phys. Rev. D **82** (2010), 072004 [arXiv:1007.0504 [hep-ex]].
- [15] A. Poluektov *et al.* [Belle], Phys. Rev. D **81** (2010), 112002 [arXiv:1003.3360 [hep-ex]].
- [16] R. Aaij *et al.* [LHCb], Phys. Rev. Lett. **108** (2012), 101803 [arXiv:1112.3183 [hep-ex]].
- [17] R. Aaij *et al.* [LHCb], Phys. Lett. B **712** (2012), 203-212 [erratum: Phys. Lett. B **713** (2012), 351] [arXiv:1203.3662 [hep-ex]].
- [18] R. Aaij *et al.* [LHCb], Phys. Rev. Lett. **110** (2013) no.22, 221601 [arXiv:1304.6173 [hep-ex]].
- [19] R. Aaij *et al.* [LHCb], JHEP **07** (2014), 041 [arXiv:1405.2797 [hep-ex]].
- [20] R. Aaij *et al.* [LHCb], Phys. Rev. Lett. **122** (2019) no.21, 211803 [arXiv:1903.08726 [hep-ex]].
- [21] M. Ablikim *et al.* [BESIII], Chin. Phys. C **44** (2020) no.4, 040001 [arXiv:1912.05983 [hep-ex]].
- [22] E. Kou *et al.* [Belle-II], PTEP **2019** (2019) no.12, 123C01 [erratum: PTEP **2020** (2020) no.2, 029201] [arXiv:1808.10567 [hep-ex]].
- [23] R. Aaij *et al.* [LHCb], Eur. Phys. J. C **73** (2013) no.4, 2373 [arXiv:1208.3355 [hep-ex]].
- [24] R. Aaij *et al.* [LHCb], [arXiv:1808.08865 [hep-ex]].
- [25] R. Aaij *et al.* [LHCb], [arXiv:2305.10515 [hep-ex]].
- [26] M. Beneke, G. Buchalla, M. Neubert and C. T. Sachrajda, Phys. Rev. Lett. **83** (1999), 1914-1917 [arXiv:hep-ph/9905312 [hep-ph]].
- [27] M. Beneke, G. Buchalla, M. Neubert and C. T. Sachrajda, Nucl. Phys. B **591** (2000), 313-418 [arXiv:hep-ph/0006124 [hep-ph]].
- [28] Y. Y. Keum, H. N. Li and A. I. Sanda, Phys. Rev. D **63** (2001), 054008 [arXiv:hep-ph/0004173 [hep-ph]].
- [29] C. D. Lu, K. Ukai and M. Z. Yang, Phys. Rev. D **63** (2001), 074009 [arXiv:hep-ph/0004213 [hep-ph]].
- [30] C. W. Bauer, S. Fleming, D. Pirjol and I. W. Stewart, Phys. Rev. D **63** (2001), 114020 [arXiv:hep-ph/0011336 [hep-ph]].
- [31] C. W. Bauer, D. Pirjol and I. W. Stewart, Phys. Rev. D **65** (2002), 054022 [arXiv:hep-ph/0109045 [hep-ph]].
- [32] H. n. Li, C. D. Lu and F. S. Yu, Phys. Rev. D **86** (2012), 036012 [arXiv:1203.3120 [hep-ph]].
- [33] Q. Qin, H. n. Li, C. D. Lü and F. S. Yu, Phys. Rev. D **89** (2014) no.5, 054006 [arXiv:1305.7021 [hep-ph]].
- [34] Q. Qin, Z. T. Zou, X. Yu, H. n. Li and C. D. Lü, Phys. Lett. B **732** (2014), 36-40 [arXiv:1401.1028 [hep-ph]].
- [35] Q. Qin, C. Wang, D. Wang and S. H. Zhou, Front. Phys. (Beijing) **18** (2023) no.6, 64602 [arXiv:2111.14472 [hep-ph]].
- [36] F. S. Yu, D. Wang and H. n. Li, Phys. Rev. Lett. **119** (2017) no.18, 181802 [arXiv:1707.09297 [hep-ph]].
- [37] Y. F. Shen, W. J. Song and Q. Qin, [arXiv:2301.05848 [hep-ph]].
- [38] R. L. Workman *et al.* [Particle Data Group], PTEP **2022** (2022), 083C01

- [39] Y. S. Amhis *et al.* [HFLAV], Phys. Rev. D **107** (2023) no.5, 052008 [arXiv:2206.07501 [hep-ex]].
- [40] Y. I. Azimov, [arXiv:hep-ph/9712288 [hep-ph]].
- [41] R. Aaij *et al.* [LHCb], JHEP **06** (2015), 131 [arXiv:1503.07055 [hep-ex]].
- [42] B. Aubert *et al.* [BaBar], Phys. Rev. D **79** (2009), 072003 [arXiv:0805.2001 [hep-ex]].
- [43] P. Krokovny *et al.* [Belle], Phys. Rev. Lett. **90** (2003), 141802 [arXiv:hep-ex/0212066 [hep-ex]].
- [44] B. Aubert *et al.* [BaBar], Phys. Rev. Lett. **96** (2006), 011803 [arXiv:hep-ex/0509036 [hep-ex]].
- [45] B. Aubert *et al.* [BaBar], Phys. Rev. D **74** (2006), 031101 [arXiv:hep-ex/0604016 [hep-ex]].
- [46] R. Aaij *et al.* [LHCb], JHEP **08** (2016), 137 [arXiv:1605.01082 [hep-ex]].
- [47] R. Aaij *et al.* [LHCb], JHEP **06** (2016), 131 [arXiv:1604.01525 [hep-ex]].
- [48] T. Aaltonen *et al.* [CDF], Phys. Rev. D **83** (2011), 052012 [arXiv:1102.1961 [hep-ex]].
- [49] R. Aaij *et al.* [LHCb], Phys. Lett. B **706** (2011), 32-39 [arXiv:1110.3676 [hep-ex]].
- [50] R. Aaij *et al.* [LHCb], Phys. Rev. D **90** (2014) no.7, 072003 [arXiv:1407.7712 [hep-ex]].
- [51] R. Aaij *et al.* [LHCb], Phys. Rev. D **90** (2014) no.11, 112002 [arXiv:1407.8136 [hep-ex]].

A Formulae for Category 3

Here we present relevant analytical expressions for the terms of the double-mixing CP violation of **Category 3** in Section 2. Based on the definitions of the parameters provided in (2.26), we can derive the individual terms in (2.4) as

$$\begin{aligned}
C_+(t_2) = e^{-\Gamma_2 t_2} \Bigg\{ & r_2 \sinh \frac{\Delta\Gamma_2 t_2}{2} \left[r_1^2 \left(\left| \frac{q_2}{p_2} \right| \cos \Omega_3 - \left| \frac{p_2}{q_2} \right| \cos \Omega_4 \right) + \left| \frac{p_2}{q_2} \right| \cos \Omega_3 - \left| \frac{q_2}{p_2} \right| \cos \Omega_4 \right] \\
& - r_2 \sin \Delta m_2 t_2 \left[r_1^2 \left(\left| \frac{q_2}{p_2} \right| \sin \Omega_3 - \left| \frac{p_2}{q_2} \right| \sin \Omega_4 \right) - \left| \frac{p_2}{q_2} \right| \sin \Omega_3 + \left| \frac{q_2}{p_2} \right| \sin \Omega_4 \right] \\
& + r_1 \sinh \frac{\Delta\Gamma_2 t_2}{2} \left[r_2^2 \left(\left| \frac{q_2}{p_2} \right| \cos \Omega_1 - \left| \frac{p_2}{q_2} \right| \cos \Omega_2 \right) + \left| \frac{p_2}{q_2} \right| \cos \Omega_1 - \left| \frac{q_2}{p_2} \right| \cos \Omega_2 \right] \\
& - r_1 \sin \Delta m_2 t_2 \left[r_2^2 \left(\left| \frac{q_2}{p_2} \right| \sin \Omega_1 - \left| \frac{p_2}{q_2} \right| \sin \Omega_2 \right) - \left| \frac{p_2}{q_2} \right| \sin \Omega_1 + \left| \frac{q_2}{p_2} \right| \sin \Omega_2 \right] \Bigg\} \\
& + 2r_1 r_2 |g_{+,2}(t_2)|^2 \left[\cos(\Omega_1 - \Omega_3) - \cos(\Omega_2 - \Omega_4) \right] \\
& + 2r_1 r_2 |g_{-,2}(t_2)|^2 \left[\cos(\Omega_1 + \Omega_3) - \cos(\Omega_2 + \Omega_4) \right] \\
& + (r_1^2 r_2^2 - 1) |g_{-,2}(t_2)|^2 \left(\left| \frac{q_2}{p_2} \right|^2 - \left| \frac{p_2}{q_2} \right|^2 \right), \tag{A.1}
\end{aligned}$$

where $\Omega_1 \equiv \delta_1 + \theta_1 - \phi_2$, $\Omega_2 \equiv \delta_1 - \theta_1 + \phi_2$, $\Omega_3 \equiv \delta_2 - \phi_2$ and $\Omega_4 \equiv \delta_2 + \phi_2$,

$$C_-(t_2) = |g_{-,2}(t_2)|^2 \left\{ r_1^2 \left(\left| \frac{q_1}{p_1} \right|^2 \left| \frac{p_2}{q_2} \right|^2 - \left| \frac{p_1}{q_1} \right|^2 \left| \frac{q_2}{p_2} \right|^2 \right) + r_2^2 \left(\left| \frac{q_1}{p_1} \right|^2 \left| \frac{q_2}{p_2} \right|^2 - \left| \frac{p_1}{q_1} \right|^2 \left| \frac{p_2}{q_2} \right|^2 \right) \right\}$$

$$\begin{aligned}
& + 2r_1 r_2 \left| \frac{q_1}{p_1} \right|^2 \left\{ |g_{+,2}(t_2)|^2 \cos(\Omega_2 + \Omega_3) + |g_{-,2}(t_2)|^2 \cos(\Omega_2 - \Omega_3) \right\} \\
& - 2r_1 r_2 \left| \frac{p_1}{q_1} \right|^2 \left\{ |g_{+,2}(t_2)|^2 \cos(\Omega_1 + \Omega_4) + |g_{-,2}(t_2)|^2 \cos(\Omega_1 - \Omega_4) \right\} \\
& + e^{-\Gamma_2 t_2} \left\{ r_2 \left| \frac{q_1}{p_1} \right|^2 \left| \frac{q_2}{p_2} \right|^2 \left(\sinh \frac{\Delta \Gamma_2 t_2}{2} \cos \Omega_3 - \sin \Delta m_2 t_2 \sin \Omega_3 \right) \right. \\
& + r_1^2 r_2 \left| \frac{q_1}{p_1} \right|^2 \left| \frac{p_2}{q_2} \right|^2 \left(\sinh \frac{\Delta \Gamma_2 t_2}{2} \cos \Omega_3 + \sin \Delta m_2 t_2 \sin \Omega_3 \right) \\
& - r_2 \left| \frac{p_1}{q_1} \right|^2 \left| \frac{p_2}{q_2} \right|^2 \left(\sinh \frac{\Delta \Gamma_2 t_2}{2} \cos \Omega_4 - \sin \Delta m_2 t_2 \sin \Omega_4 \right) \\
& - r_1^2 r_2 \left| \frac{p_1}{q_1} \right|^2 \left| \frac{q_2}{p_2} \right|^2 \left(\sinh \frac{\Delta \Gamma_2 t_2}{2} \cos \Omega_4 + \sin \Delta m_2 t_2 \sin \Omega_4 \right) \\
& + r_1 \sinh \frac{\Delta \Gamma_2 t_2}{2} \left[\left| \frac{q_1}{p_1} \right|^2 \cos \Omega_2 \left(r_2^2 \left| \frac{q_2}{p_2} \right| + \left| \frac{p_2}{q_2} \right| \right) - \left| \frac{p_1}{q_1} \right|^2 \cos \Omega_1 \left(r_2^2 \left| \frac{p_2}{q_2} \right| + \left| \frac{q_2}{p_2} \right| \right) \right] \\
& + r_1 \sin \Delta m_2 t_2 \left[\left| \frac{q_1}{p_1} \right|^2 \sin \Omega_2 \left(r_2^2 \left| \frac{q_2}{p_2} \right| - \left| \frac{p_2}{q_2} \right| \right) - \left| \frac{p_1}{q_1} \right|^2 \sin \Omega_1 \left(r_2^2 \left| \frac{p_2}{q_2} \right| - \left| \frac{q_2}{p_2} \right| \right) \right] \Big\} \\
& + (r_1^2 r_2^2 + 1) \left(\left| \frac{q_1}{p_1} \right|^2 - \left| \frac{p_1}{q_1} \right|^2 \right) |g_{+,2}(t_2)|^2, \tag{A.2}
\end{aligned}$$

$$\begin{aligned}
S_{n,1}(t_2) = & \frac{e^{-\Gamma_2 t_2}}{2} \left\{ g(-, -, -, -) \times \sinh \frac{\Delta \Gamma_2 t_2}{2} \left[r_1^2 \sin(\Omega_5 - 2\Omega_6) + \sin \Omega_5 \right] \right. \\
& + g(-, +, -, +) \times \sin \Delta m_2 t_2 \left[r_1^2 \cos(\Omega_5 - 2\Omega_6) - \cos \Omega_5 \right] \Big\} \\
& + r_1 r_2 \left| \frac{q_2}{p_2} \right| \sin(\delta_1 - \Omega_5 + \Omega_6) e^{-\Gamma_2 t_2} \left\{ \left| \frac{q_1}{p_1} \right| \left[\sinh \frac{\Delta \Gamma_2 t_2}{2} \cos \Omega_3 - \sin \Delta m_2 t_2 \sin \Omega_3 \right] \right. \\
& + \left| \frac{p_1}{q_1} \right| \left[\sinh \frac{\Delta \Gamma_2 t_2}{2} \cos \Omega_4 + \sin \Delta m_2 t_2 \sin \Omega_4 \right] \Big\} \\
& - r_1 r_2 \left| \frac{p_2}{q_2} \right| \sin(\delta_1 + \Omega_5 - \Omega_6) e^{-\Gamma_2 t_2} \left\{ \left| \frac{q_1}{p_1} \right| \left[\sinh \frac{\Delta \Gamma_2 t_2}{2} \cos \Omega_3 + \sin \Delta m_2 t_2 \sin \Omega_3 \right] \right. \\
& + \left| \frac{p_1}{q_1} \right| \left[\sinh \frac{\Delta \Gamma_2 t_2}{2} \cos \Omega_4 - \sin \Delta m_2 t_2 \sin \Omega_4 \right] \Big\}, \tag{A.3}
\end{aligned}$$

where $\Omega_5 \equiv \theta_3 - \phi_1 - \phi_2$, $\Omega_6 \equiv \theta_1 - \phi_2$, and the $g(-, +, -, +)$ is defined as

$$g(-, +, -, +) = - \left| \frac{q_1}{p_1} \right| \left| \frac{p_2}{q_2} \right| + r_2^2 \left| \frac{q_1}{p_1} \right| \left| \frac{q_2}{p_2} \right| - r_2^2 \left| \frac{p_1}{q_1} \right| \left| \frac{p_2}{q_2} \right| + \left| \frac{p_1}{q_1} \right| \left| \frac{q_2}{p_2} \right|,$$

and others g functions with different sign arguments can be obtained by flip signs in the above expression accordingly,

$$\begin{aligned}
S_{n,2}(t_2) = & - r_1^2 r_2 \left| \frac{q_1}{p_1} \right| \left\{ |g_{+,2}(t_2)|^2 \sin(\Omega_3 + \Omega_5 - 2\Omega_6) - |g_{-,2}(t_2)|^2 \sin(\Omega_3 - \Omega_5 + 2\Omega_6) \right\} \\
& + r_2 \left| \frac{q_1}{p_1} \right| \left\{ |g_{+,2}(t_2)|^2 \sin(\Omega_3 - \Omega_5) - |g_{-,2}(t_2)|^2 \sin(\Omega_3 + \Omega_5) \right\}
\end{aligned}$$

$$\begin{aligned}
& + r_1^2 r_2 \left| \frac{p_1}{q_1} \right| \left\{ |g_{+,2}(t_2)|^2 \sin(\Omega_4 - \Omega_5 + 2\Omega_6) - |g_{-,2}(t_2)|^2 \sin(\Omega_4 + \Omega_5 - 2\Omega_6) \right\} \\
& - r_2 \left| \frac{p_1}{q_1} \right| \left\{ |g_{+,2}(t_2)|^2 \sin(\Omega_4 + \Omega_5) - |g_{-,2}(t_2)|^2 \sin(\Omega_4 - \Omega_5) \right\} \\
& + r_1 \sin(\delta_1 - \Omega_5 + \Omega_6) f_1(q, p) - r_1 \sin(\delta_1 + \Omega_5 - \Omega_6) f_1(p, q), \tag{A.4}
\end{aligned}$$

where

$$f_1(q, p) = |g_{+,2}(t_2)|^2 \left(\left| \frac{q_1}{p_1} \right| + r_2^2 \left| \frac{p_1}{q_1} \right| \right) + \left| \frac{q_2}{p_2} \right|^2 |g_{-,2}(t_2)|^2 \left(r_2^2 \left| \frac{q_1}{p_1} \right| + \left| \frac{p_1}{q_1} \right| \right),$$

and the function $f_1(p, q)$ is obtained by exchanging $p_{1,2} \leftrightarrow q_{1,2}$ in $f_1(q, p)$,

$$\begin{aligned}
S_{h,1}(t_2) = & \frac{e^{-\Gamma_2 t_2}}{2} \left\{ g(+, +, -, -) \sinh \frac{\Delta \Gamma_2 t_2}{2} \left[r_1^2 \cos(\Omega_5 - 2\Omega_6) + \cos \Omega_5 \right] \right. \\
& - g(+, -, -, +) \sin \Delta m_2 t_2 \left[r_1^2 \sin(\Omega_5 - 2\Omega_6) - \sin \Omega_5 \right] \Big\} \\
& + r_1 r_2 \left| \frac{q_2}{p_2} \right| \cos(\delta_1 - \Omega_5 + \Omega_6) e^{-\Gamma_2 t_2} \left\{ \left| \frac{q_1}{p_1} \right| \left[\sinh \frac{\Delta \Gamma_2 t_2}{2} \cos \Omega_3 - \sin \Delta m_2 t_2 \sin \Omega_3 \right] \right. \\
& - \left| \frac{p_1}{q_1} \right| \left[\sinh \frac{\Delta \Gamma_2 t_2}{2} \cos \Omega_4 + \sin \Delta m_2 t_2 \sin \Omega_4 \right] \Big\} \\
& + r_1 r_2 \left| \frac{p_2}{q_2} \right| \cos(\delta_1 + \Omega_5 - \Omega_6) e^{-\Gamma_2 t_2} \left\{ \left| \frac{q_1}{p_1} \right| \left[\sinh \frac{\Delta \Gamma_2 t_2}{2} \cos \Omega_3 + \sin \Delta m_2 t_2 \sin \Omega_3 \right] \right. \\
& - \left| \frac{p_1}{q_1} \right| \left[\sinh \frac{\Delta \Gamma_2 t_2}{2} \cos \Omega_4 - \sin \Delta m_2 t_2 \sin \Omega_4 \right] \Big\}, \tag{A.5}
\end{aligned}$$

$$\begin{aligned}
S_{h,2}(t_2) = & r_1^2 r_2 \left| \frac{q_1}{p_1} \right| \left[|g_{+,2}(t_2)|^2 \cos(\Omega_3 + \Omega_5 - 2\Omega_6) + |g_{-,2}(t_2)|^2 \cos(\Omega_3 - \Omega_5 + 2\Omega_6) \right] \\
& + r_2 \left| \frac{q_1}{p_1} \right| \left[|g_{+,2}(t_2)|^2 \cos(\Omega_3 - \Omega_5) + |g_{-,2}(t_2)|^2 \cos(\Omega_3 + \Omega_5) \right] \\
& - r_1^2 r_2 \left| \frac{p_1}{q_1} \right| \left[|g_{+,2}(t_2)|^2 \cos(\Omega_4 - \Omega_5 + 2\Omega_6) + |g_{-,2}(t_2)|^2 \cos(\Omega_4 + \Omega_5 - 2\Omega_6) \right] \\
& - r_2 \left| \frac{p_1}{q_1} \right| \left[|g_{+,2}(t_2)|^2 \cos(\Omega_4 + \Omega_5) + |g_{-,2}(t_2)|^2 \cos(\Omega_4 - \Omega_5) \right] \\
& + r_1 \cos(\delta_1 - \Omega_5 + \Omega_6) f_2(q, p) + r_1 \cos(\delta_1 + \Omega_5 - \Omega_6) f_2(p, q), \tag{A.6}
\end{aligned}$$

where

$$f_2(q, p) = |g_{+,2}(t_2)|^2 \left(\left| \frac{q_1}{p_1} \right| - r_2^2 \left| \frac{p_1}{q_1} \right| \right) + \left| \frac{q_2}{p_2} \right|^2 |g_{-,2}(t_2)|^2 \left(r_2^2 \left| \frac{q_1}{p_1} \right| - \left| \frac{p_1}{q_1} \right| \right),$$

and the function $f_2(p, q)$ is obtained by exchanging $p_{1,2} \leftrightarrow q_{1,2}$ in $f_2(q, p)$,

$$\begin{aligned}
C'_+(t_2) = & e^{-\Gamma_2 t_2} \left\{ r_2 \sinh \frac{\Delta \Gamma_2 t_2}{2} \left[r_1^2 \left(\left| \frac{q_2}{p_2} \right| \cos \Omega_3 + \left| \frac{p_2}{q_2} \right| \cos \Omega_4 \right) + \left| \frac{p_2}{q_2} \right| \cos \Omega_3 + \left| \frac{q_2}{p_2} \right| \cos \Omega_4 \right] \right. \\
& - r_2 \sin \Delta m_2 t_2 \left[r_1^2 \left(\left| \frac{q_2}{p_2} \right| \sin \Omega_3 + \left| \frac{p_2}{q_2} \right| \sin \Omega_4 \right) - \left| \frac{p_2}{q_2} \right| \sin \Omega_3 - \left| \frac{q_2}{p_2} \right| \sin \Omega_4 \right] \Big\}
\end{aligned}$$

$$\begin{aligned}
& +r_1 \sinh \frac{\Delta\Gamma_2 t_2}{2} \left[r_2^2 \left(\left| \frac{q_2}{p_2} \right| \cos \Omega_1 + \left| \frac{p_2}{q_2} \right| \cos \Omega_2 \right) + \left| \frac{p_2}{q_2} \right| \cos \Omega_1 + \left| \frac{q_2}{p_2} \right| \cos \Omega_2 \right] \\
& -r_1 \sin \Delta m_2 t_2 \left[r_2^2 \left(\left| \frac{q_2}{p_2} \right| \sin \Omega_1 + \left| \frac{p_2}{q_2} \right| \sin \Omega_2 \right) - \left| \frac{p_2}{q_2} \right| \sin \Omega_1 - \left| \frac{q_2}{p_2} \right| \sin \Omega_2 \right] \\
& + 2r_1 r_2 |g_{+,2}(t_2)|^2 \left[\cos(\Omega_1 - \Omega_3) + \cos(\Omega_2 - \Omega_4) \right] \\
& + 2r_1 r_2 |g_{-,2}(t_2)|^2 \left[\cos(\Omega_1 + \Omega_3) + \cos(\Omega_2 + \Omega_4) \right] \\
& + (r_1^2 r_2^2 + 1) |g_{-,2}(t_2)|^2 \left(\left| \frac{q_2}{p_2} \right|^2 + \left| \frac{p_2}{q_2} \right|^2 \right) + 2(r_1^2 + r_2^2) |g_{+,2}(t_2)|^2, \tag{A.7}
\end{aligned}$$

$$\begin{aligned}
C'_-(t_2) = & |g_{-,2}(t_2)|^2 \left\{ r_1^2 \left(\left| \frac{q_1}{p_1} \right|^2 \left| \frac{p_2}{q_2} \right|^2 + \left| \frac{p_1}{q_1} \right|^2 \left| \frac{q_2}{p_2} \right|^2 \right) + r_2^2 \left(\left| \frac{q_1}{p_1} \right|^2 \left| \frac{q_2}{p_2} \right|^2 + \left| \frac{p_1}{q_1} \right|^2 \left| \frac{p_2}{q_2} \right|^2 \right) \right\} \\
& + 2r_1 r_2 \left| \frac{q_1}{p_1} \right|^2 \left[|g_{+,2}(t_2)|^2 \cos(\Omega_2 + \Omega_3) + |g_{-,2}(t_2)|^2 \cos(\Omega_2 - \Omega_3) \right] \\
& + 2r_1 r_2 \left| \frac{p_1}{q_1} \right|^2 \left[|g_{+,2}(t_2)|^2 \cos(\Omega_1 + \Omega_4) + |g_{-,2}(t_2)|^2 \cos(\Omega_1 - \Omega_4) \right] \\
& + e^{-\Gamma_2 t_2} \left\{ r_2 \left| \frac{q_1}{p_1} \right|^2 \left| \frac{q_2}{p_2} \right| \left(\sinh \frac{\Delta\Gamma_2 t_2}{2} \cos \Omega_3 - \sin \Delta m_2 t_2 \sin \Omega_3 \right) \right. \\
& + r_1^2 r_2 \left| \frac{q_1}{p_1} \right|^2 \left| \frac{p_2}{q_2} \right| \left(\sinh \frac{\Delta\Gamma_2 t_2}{2} \cos \Omega_3 + \sin \Delta m_2 t_2 \sin \Omega_3 \right) \\
& + r_2 \left| \frac{p_1}{q_1} \right|^2 \left| \frac{p_2}{q_2} \right| \left(\sinh \frac{\Delta\Gamma_2 t_2}{2} \cos \Omega_4 - \sin \Delta m_2 t_2 \sin \Omega_4 \right) \\
& + r_1^2 r_2 \left| \frac{p_1}{q_1} \right|^2 \left| \frac{q_2}{p_2} \right| \left(\sinh \frac{\Delta\Gamma_2 t_2}{2} \cos \Omega_4 + \sin \Delta m_2 t_2 \sin \Omega_4 \right) \\
& + r_1 \sinh \frac{\Delta\Gamma_2 t_2}{2} \left[\left| \frac{q_1}{p_1} \right|^2 \cos \Omega_2 \left(r_2^2 \left| \frac{q_2}{p_2} \right| + \left| \frac{p_2}{q_2} \right| \right) + \left| \frac{p_1}{q_1} \right|^2 \cos \Omega_1 \left(r_2^2 \left| \frac{p_2}{q_2} \right| + \left| \frac{q_2}{p_2} \right| \right) \right] \\
& + r_1 \sin \Delta m_2 t_2 \left[\left| \frac{q_1}{p_1} \right|^2 \sin \Omega_2 \left(r_2^2 \left| \frac{q_2}{p_2} \right| - \left| \frac{p_2}{q_2} \right| \right) + \left| \frac{p_1}{q_1} \right|^2 \sin \Omega_1 \left(r_2^2 \left| \frac{p_2}{q_2} \right| - \left| \frac{q_2}{p_2} \right| \right) \right] \Bigg\} \\
& + (r_1^2 r_2^2 + 1) \left(\left| \frac{q_1}{p_1} \right|^2 + \left| \frac{p_1}{q_1} \right|^2 \right) |g_{+,2}(t_2)|^2, \tag{A.8}
\end{aligned}$$

$$\begin{aligned}
S'_{n,1}(t_2) = & \frac{e^{-\Gamma_2 t_2}}{2} \left\{ g(-, -, +, +) \times \sinh \frac{\Delta\Gamma_2 t_2}{2} \left[r_1^2 \sin(\Omega_5 - 2\Omega_6) + \sin \Omega_5 \right] \right. \\
& + g(-, +, +, -) \times \sin \Delta m_2 t_2 \left[r_1^2 \cos(\Omega_5 - 2\Omega_6) - \cos \Omega_5 \right] \Bigg\} \\
& + r_1 r_2 \left| \frac{q_2}{p_2} \right| \sin(\delta_1 - \Omega_5 + \Omega_6) e^{-\Gamma_2 t_2} \left\{ \left| \frac{q_1}{p_1} \right| \left[\sinh \frac{\Delta\Gamma_2 t_2}{2} \cos \Omega_3 - \sin \Delta m_2 t_2 \sin \Omega_3 \right] \right. \\
& \left. \left. - \left| \frac{p_1}{q_1} \right| \left[\sinh \frac{\Delta\Gamma_2 t_2}{2} \cos \Omega_4 + \sin \Delta m_2 t_2 \sin \Omega_4 \right] \right\}
\end{aligned}$$

$$\begin{aligned}
& -r_1 r_2 \left| \frac{p_2}{q_2} \right| \sin(\delta_1 + \Omega_5 - \Omega_6) e^{-\Gamma_2 t_2} \left\{ \left| \frac{q_1}{p_1} \right| \left[\sinh \frac{\Delta \Gamma_2 t_2}{2} \cos \Omega_3 + \sin \Delta m_2 t_2 \sin \Omega_3 \right] \right. \\
& \left. - \left| \frac{p_1}{q_1} \right| \left[\sinh \frac{\Delta \Gamma_2 t_2}{2} \cos \Omega_4 - \sin \Delta m_2 t_2 \sin \Omega_4 \right] \right\}, \tag{A.9}
\end{aligned}$$

$$\begin{aligned}
S'_{n,2}(t_2) = & -r_1^2 r_2 \left| \frac{q_1}{p_1} \right| \left\{ |g_{+,2}(t_2)|^2 \sin(\Omega_3 + \Omega_5 - 2\Omega_6) - |g_{-,2}(t_2)|^2 \sin(\Omega_3 - \Omega_5 + 2\Omega_6) \right\} \\
& + r_2 \left| \frac{q_1}{p_1} \right| \left\{ |g_{+,2}(t_2)|^2 \sin(\Omega_3 - \Omega_5) - |g_{-,2}(t_2)|^2 \sin(\Omega_3 + \Omega_5) \right\} \\
& - r_1^2 r_2 \left| \frac{p_1}{q_1} \right| \left\{ |g_{+,2}(t_2)|^2 \sin(\Omega_4 - \Omega_5 + 2\Omega_6) - |g_{-,2}(t_2)|^2 \sin(\Omega_4 + \Omega_5 - 2\Omega_6) \right\} \\
& + r_2 \left| \frac{p_1}{q_1} \right| \left\{ |g_{+,2}(t_2)|^2 \sin(\Omega_4 + \Omega_5) + |g_{-,2}(t_2)|^2 \sin(\Omega_4 - \Omega_5) \right\} \\
& + r_1 \sin(\delta_1 - \Omega_5 + \Omega_6) f_2(q, p) - r_1 \sin(\delta_1 + \Omega_5 - \Omega_6) f_2(p, q), \tag{A.10}
\end{aligned}$$

$$\begin{aligned}
S'_{h,1}(t_2) = & \frac{e^{-\Gamma_2 t_2}}{2} \left\{ g(+, +, +, +) \sinh \frac{\Delta \Gamma_2 t_2}{2} \left[r_1^2 \cos(\Omega_5 - 2\Omega_6) + \cos \Omega_5 \right] \right. \\
& \left. - g(+, -, +, -) \sin \Delta m_2 t_2 \left[r_1^2 \sin(\Omega_5 - 2\Omega_6) - \sin \Omega_5 \right] \right\} \\
& + r_1 r_2 \left| \frac{q_2}{p_2} \right| \cos(\delta_1 - \Omega_5 + \Omega_6) e^{-\Gamma_2 t_2} \left\{ \left| \frac{q_1}{p_1} \right| \left[\sinh \frac{\Delta \Gamma_2 t_2}{2} \cos \Omega_3 - \sin \Delta m_2 t_2 \sin \Omega_3 \right] \right. \\
& \left. + \left| \frac{p_1}{q_1} \right| \left[\sinh \frac{\Delta \Gamma_2 t_2}{2} \cos \Omega_4 + \sin \Delta m_2 t_2 \sin \Omega_4 \right] \right\} \\
& + r_1 r_2 \left| \frac{p_2}{q_2} \right| \cos(\delta_1 + \Omega_5 - \Omega_6) e^{-\Gamma_2 t_2} \left\{ \left| \frac{q_1}{p_1} \right| \left[\sinh \frac{\Delta \Gamma_2 t_2}{2} \cos \Omega_3 + \sin \Delta m_2 t_2 \sin \Omega_3 \right] \right. \\
& \left. + \left| \frac{p_1}{q_1} \right| \left[\sinh \frac{\Delta \Gamma_2 t_2}{2} \cos \Omega_4 - \sin \Delta m_2 t_2 \sin \Omega_4 \right] \right\}, \tag{A.11}
\end{aligned}$$

$$\begin{aligned}
S'_{h,2}(t_2) = & r_1^2 r_2 \left| \frac{q_1}{p_1} \right| \left[|g_{+,2}(t_2)|^2 \cos(\Omega_3 + \Omega_5 - 2\Omega_6) + |g_{-,2}(t_2)|^2 \cos(\Omega_3 - \Omega_5 + 2\Omega_6) \right] \\
& + r_2 \left| \frac{q_1}{p_1} \right| \left\{ |g_{+,2}(t_2)|^2 \cos(\Omega_3 - \Omega_5) + |g_{-,2}(t_2)|^2 \cos(\Omega_3 + \Omega_5) \right\} \\
& + r_1^2 r_2 \left| \frac{p_1}{q_1} \right| \left[|g_{+,2}(t_2)|^2 \cos(\Omega_4 - \Omega_5 + 2\Omega_6) + |g_{-,2}(t_2)|^2 \cos(\Omega_4 + \Omega_5 - 2\Omega_6) \right] \\
& + r_2 \left| \frac{p_1}{q_1} \right| \left\{ |g_{+,2}(t_2)|^2 \cos(\Omega_4 + \Omega_5) + |g_{-,2}(t_2)|^2 \cos(\Omega_4 - \Omega_5) \right\} \\
& + r_1 \cos(\delta_1 - \Omega_5 + \Omega_6) f_1(q, p) + r_1 \cos(\delta_1 + \Omega_5 - \Omega_6) f_1(p, q). \tag{A.12}
\end{aligned}$$